Primary-Side Deposits on PWR Steam Generator Tubes

NP-2968
Research Project 825-2

Interim Report, March 1983

Prepared by

WESTINGHOUSE ELECTRIC CORPORATION
Nuclear Technology Division
P.O. Box 355
Pittsburgh, Pennsylvania 15230

Principal Investigators
C. A. Bergmann
J. Roesmer
D. W. Perone

Prepared for

Electric Power Research Institute
3412 Hillview Avenue
Palo Alto, California 94304

EPRI Project Manager
R. A. Shaw

Chemistry, Radiation, and Monitoring Program
Nuclear Power Division

ORDERING INFORMATION

Requests for copies of this report should be directed to Research Reports Center (RRC), Box 50490, Palo Alto, CA 94303, (415) 965-4081. There is no charge for reports requested by EPRI member utilities and affiliates, U.S. utility associations, U.S. government agencies (federal, state, and local), media, and foreign organizations with which EPRI has an information exchange agreement. On request, RRC will send a catalog of EPRI reports.

NOTICE

Prepared by
Westinghouse Electric Corporation
Pittsburgh, Pennsylvania

EPRI PERSPECTIVE

PROJECT DESCRIPTION

The operational and design factors that most influence radiation buildup in PWRs are not well specified. Most of the radioisotopes that produce these radiation fields reside on the core or on steam generator surfaces. Further insight into the nature of these deposits gives additional clues on these influencing factors.

PROJECT OBJECTIVE

This interim report describes the portion of this project (RP825-2) with the objective of determining (1) the chemical nature of the oxide deposits on the primary side of steam generator tubes and (2) the radioisotopes incorporated in those deposits.

PROJECT RESULTS

Analyses were performed on sections of steam generator tubes from eight plants. The deposited oxide film is enriched in chromium over the Inconel 600 tube material and is most likely a mixture of iron-nickel-chromite and metallic nickel. This film is quite distinctive from the fuel deposits that are nickel-ferrite combinations and is important in decontamination considerations. The cobalt concentrations in the tube oxide films are about an order of magnitude higher than in the tube material, a significant consideration in the search for cobalt sources in PWRs. This leads me to conclude that the Inconel 600 tubes are probably not as significant a source of cobalt as previously reported in EPRI Final Report NP-2681. This issue is being addressed directly in RP2008, a current project.

All the radioisotopes on the tubes are incorporated in the oxides. There is not a good correlation between the fields in the steam generator channel heads and the concentration in the oxides of Co-60, the principal contributor to the radiation fields. This is consistent with other results showing that the tube deposits are not a major contributor to channel-head fields.

This report is relevant to plant chemists, decontamination engineers, and those involved in ALARA programs.

Robert A. Shaw, Project Manager
Nuclear Power Division

ABSTRACT

The evaluation of analyses of material removed from primary side steam generator tubing samples taken from nuclear plants that had operated for up to 7 effective full power years are presented in this report. The types of analyses included radiochemical, chemical, scanning electron microscope (SEM), and energy dispersive X-ray (EDAX) techniques to characterize the surfaces and composition of the tubing material. An evaluation of the data obtained and a comparison with in-core crud data and with values calculated by a mathematical activity transport model (CORA) are also given in the report.

ACKNOWLEDGMENTS

The authors wish to acknowledge the considerable assistance of Messrs. C. A. Blackburn, R. W. McKinney, L. Zuckett and Z. L. Kardos, who performed the radiochemical, chemical, SEM/EDAX, and atomic absorption analyses of the tubing materials presented and discussed in this report. The constructive comments of Y. Solomon, J. Corbett, and Dr. S. Kang, who reviewed the report, are appreciated as well as the efforts of Ms. J. G. Nagle who edited the report. Lastly, the support and comments of the EPRI Project Manager, Dr. R. A. Shaw, are appreciated.

CONTENTS

ILLUSTRATIONS

TABLES

SUMMARY

A considerable amount of radiochemical and chemical data have been obtained from in-core crud in nuclear plants, but little comparable data have been taken from out-of-core surfaces in Westinghouse-designed plants. Samples of tubes from a number of steam generators had been removed and analyzed for various reasons during the past 10 years.

Since data from these tubes could provide unique information concerning out-of-core crud as a function of plant operation, a program was established under an EPRI contract to retrieve such tubes from storage, choose representative samples, and perform analyses of the material removed. The types of analyses included radiochemical, chemical, scanning electron microscope (SEM), and energy dispersive X-ray (EDAX) techniques to characterize the surfaces and composition of the tubing crud. The data obtained from the analyses will provide additional insight into crud transport and deposition phenomena.

Although the activity on the tubing surface was found to be generally quite uniform, radiation surveys and visual examinations were used to assure that representative samples of the tubing were taken -- in particular for those to be destructively analyzed. A total of 19 tubes were selected for in situ radioactivity measurement and six were chosen for electrochemical descaling of the tube inner surface.

It was found that the Co-60 on the tubes increased with time of plant operation up to about 9 effective full power years. This trend is similar to that calculated by the CORA mathematical activity transport model except that the observed values were about 50 percent greater. The crud specific activity of Fe-55, Co-60, and Mn-54 in the descaled material decreased with operating time. This same trend was calculated by the CORA code, although the absolute values did not agree for the various nuclides.

The chemical composition of the material descaled from the tubes approached that of the Inconel tubing as subsequent descalings (up to three) were made. Most of

the material and activity was removed in the first descaling. The concentration of nickel increased with plant operating time, while that of chromium decreased with time. The percentage of iron remained about the same. The nickel-to-iron ratio in the tubing descaled material was about 1.0 compared to a ratio of 0.5 in typical core crud. The percentage of cobalt in the descaled material was about ten times that in the Inconel tubing.

The surface concentration of the descaled material was found to increase at a rate of 0.70 mg/dm^2-mo. The average thickness of the material was about 1 micron, which gave an apparent density of 3.9 g/cm^3 compared to an average value of about 1.2 g/cm^3 for core crud. SEM images of the material showed a surface of small crystallites less than 1 micron in size with cracks in the material that formed irregularly shaped agglomerates. The definition of the surface appeared to increase with exposure time.

Section 1

INTRODUCTION

BACKGROUND

As part of an EPRI program, Westinghouse is obtaining information and performing work to define radioactivity transport in the primary system of PWR nuclear plants. A considerable amount of radiochemical and chemical data have been obtained from in-core crud deposits, but little comparable data have been taken from out-of-core surfaces in Westinghouse-designed plants. Several samples of steam generator manway insert crud have been analyzed during the past several years. However, the inserts represent only a small fraction of a steam generator surface area, whereas the tubing accounts for about 60 percent of the total reactor plant surface, including the fuel surfaces. Furthermore, the inserts are not representative of the material composition of major plant areas. Thus, it is desirable to obtain tubing samples and analyze the material on the primary side surface.

Samples of tubes from a number of steam generators had been removed and analyzed for various reasons during the past 10 years. However, analyses relative to crud and activity on the tubes generally had not been performed. Since data from these tubes could provide unique information concerning out-of-core crud as a function of plant operation, a program was established under EPRI Contract 825-2 (Task 6) to retrieve such tubes from storage, choose representative samples, and perform radiochemical and chemical analyses of the material on the tubing. In addition, several tubes that had been removed from plants within the past year provided information concerning Co-58 activity that was not available from the older tubing samples. These data will assist in providing additional insight into crud transport and deposition phenomena. This report presents and evaluates the data obtained from the tubing samples.

OBJECTIVES

The objective of this work is to provide additional data to support the overall objectives of the EPRI program. The specific objectives of this program were to provide data to:

1. Determine chemical, radiochemical, and crystallographic composition of material removed from steam generator tubes

2. Define removed material morphology and variations in microstructure

3. Evaluate cobalt input to plants

4. Test future modifications of CORA transport parameters

5. Determine effects of flow changes by evaluating differences between straight and small radius U-bend sections of tube samples

6. Correlate tube data with observed plant radiation levels and possibly evaluate anomalies

SAMPLING PLAN

As a first step in the analysis program, a review of all steam generator tube samples was made to define a sampling plan and to ascertain the most appropriate samples for detailed analyses. The sampling plan was based on preferences in support of the specific objectives listed above. The preferred tubes were in general from plants that (1) were sampled before, (2) had operated for a number of effective full power years (EFPY), (3) had available both U-bends and straight length tubes, (4) had shut down recently enough to allow detection of Co-58, and (5) had shown anomalies in radiation levels between steam generators or similar units.

The sampling plan established for the steam generator tube surface material measurements is summarized in Table 1-1. The analysis type listed in the table corresponds to the following:

1. Removal of material by a descaling technique and subsequent chemical and radiochemical analyses

2. Autoradiography and SEM/EDAX analyses of material on the tubes

3. Use of a Ge(Li) detector to perform gamma ray spectroscopy of the *in situ* material

The objectives listed numerically in the table correspond to the specific objectives listed above.

Table 1-1

STEAM GENERATOR TUBE SAMPLING PLAN

Plant	Tube	SG	EFPY	Tube Shape	Analysis Type	Objectives	Remarks
A	R34C36	C	2.12	Straight	3	4	1. Sampled before in 1972
	R43C33	C	2.12	Slight curve	3	4	2. Over 7 EFPY operation
	R36C37	B	7.02	Straight	1, 2, 3	1, 2, 3, 4, 6	3. Co-58 data available
B	R1C25	D	1.75	U-bend	1, 2, 3	1, 2, 3, 4	1. Plant in Chemistry Control Experiment Program
C	R9C31	A	2.65	Straight	3	4, 6	1. Over 5 EFPY operation
	R25C47	A	3.36	Straight	3	4, 6	2. Data may explain difference between
	R45C52	B	5.35	Straight	3	4, 6	radiation levels in two SGs.
D	R1C5	A	2.09	U-bend	3	4, 5, 6	1. Data may explain difference between
	R4C30	B	2.21	Straight	3	4, 5, 6	radiation levels in two similar plants.
	R5C40	A	2.21	Straight	1, 3	1, 3, 4, 5, 6	2. Compare U-bend with straight tubes
E	R21C74	A	1.58	Straight	1, 3	1, 3, 4, 5, 6	1. Data may explain difference between
	R1C11	A	2.26	U-bend	3	4, 5, 6	radiation levels in two similar plants.
	R3C63	A	2.26	Straight	3	4, 5, 6	2. Compare U-bend with straight tubes
	R2C42	C	2.26	Straight	3	4, 5, 6	
F	R20C73	A	6.64	Straight	3	4, 6	1. Sampled before in 1972 2. Data may explain difference between radiation levels in two similar plants.
G	R18C37	A	5.96	Straight	1, 2, 3	1, 2, 3, 4, 6	1. Data may explain difference between
	R15C73	A	6.84	Straight	1, 2, 3	1, 2, 3, 4, 6	radiation levels in two similar plants. 2. Co-58 data available
H	R25C72	B	1.17	Straight	3	4, 5, 6	1. Compare U-bend with straight tube
	R1C79	B	1.90	U-Bend	3	4, 5, 6	

Section 2

EVALUATION OF IN SITU RADIOACTIVITY DATA

SELECTION OF REPRESENTATIVE TUBES

Radiation surveys and visual examinations were used to establish a representative sampling group of tubes. After completing an extensive inventory of available tubes, segments from the desired plants were surveyed either with an end-window G-M survey meter or with a collimated Ge(Li) detector system. Tube segments that had higher or lower exposure rates than typical for the tube segments from the same tube were eliminated. Lower exposure rates could be evidence of tube damage while being removed; higher rates could be local hot spots. The number of tubes eliminated was a very small part of the total sections examined.

After atypical tube segments were eliminated based on radioactivity measurements, visual examinations were performed to select samples of tubing that appeared to be in the least-handled condition. In some cases, more than one tube segment was selected for the same sample, and radioactivity measurements were performed on both segments for comparison. A total of 19 tubes were selected for in situ radioactivity measurements. For reasons described in the sampling plan, six tube samples were chosen for descaling and four tube samples were chosen for autoradiography and SEM/EDAX analysis.

VARIATION OF RADIOACTIVITY WITH EFPY

As noted above, measurement of the radioactivity on some steam generator tubes has been determined previously in 1973 on tube sections from six plants. The plants represented between 0.5 and 4.0 EFPY of operation. Table A-1 in Appendix A provides a summary of the data collected. Similar to the present program, the analysis measurements were performed using a Ge(Li) spectrometry system.

The radioactivity analysis performed on the 19 tubes described in the Task 6 original sampling plan extended the available tube data to include up to 7 EFPY. A listing of the details, the tubing sampled, the measured activity, and other pertinent information is given in Table A-2. Radioactivity data using a gamma spectrometry system were also obtained from tubing from four plants after the

activity data collection phase of the original plan was completed. These samplings provided data up to about 9 EFPY. The average values for the tubes sampled in these plants are also shown in Table A-2.

To define the statistical variation in the in situ activity, measurements were taken along the length of a tube. The measurements were obtained with a collimated Ge(Li) detector system and taken at points along tube lengths in 15 cm intervals.

The total length of the straight part of a steam generator tube is about 30 feet. The length of the samples of the steam generator tubing varied from several inches to 10 feet and represented sections of the tubing from just above the tubesheet up to the U-bends. Samples of tubing from within the tubesheet (about 2 feet long) were not available in the inventory. It was found that the standard deviation of the mean activity was typically within ±10-20 percent for measurements taken along the length of a single tube or tube segments from the same original tube.

The variation between different tubes from the same steam generator at the same removal date was also estimated. From Plant E, a 20-percent standard deviation was determined from measurements of two tubes. Tube measurements from Plant C resulted in a 15.9-percent standard deviation from one removal period, and 16.5 percent from the same steam generator 1 year later. Examples of typical tube activity measurement variations are included in Table A-3. Appendix B presents the activity data measured on all tubes surveyed.

In summary, the standard deviation of the mean activity measured on a sample of steam generator tubing is estimated to be about ± 20 percent.

Figures 2-1 through 2-3 present the in situ radioactivity data from previous and current work as a function of EFPY for Co-60 and Co-58, and their ratio. Data from both straight tubes and U-bends are included, although exclusion of the U-bend data would have no significant effect on the observations. The lines drawn on the figures are the CORA model calculated values for the total transient plus permanent out-of-core surface activity as a function of EFPY representative of a plant operating at an average power level of 100 percent (1).

Reference to the CORA computer program is made several times in this report. A detailed discussion of CORA is beyond the scope of this report; however, a brief

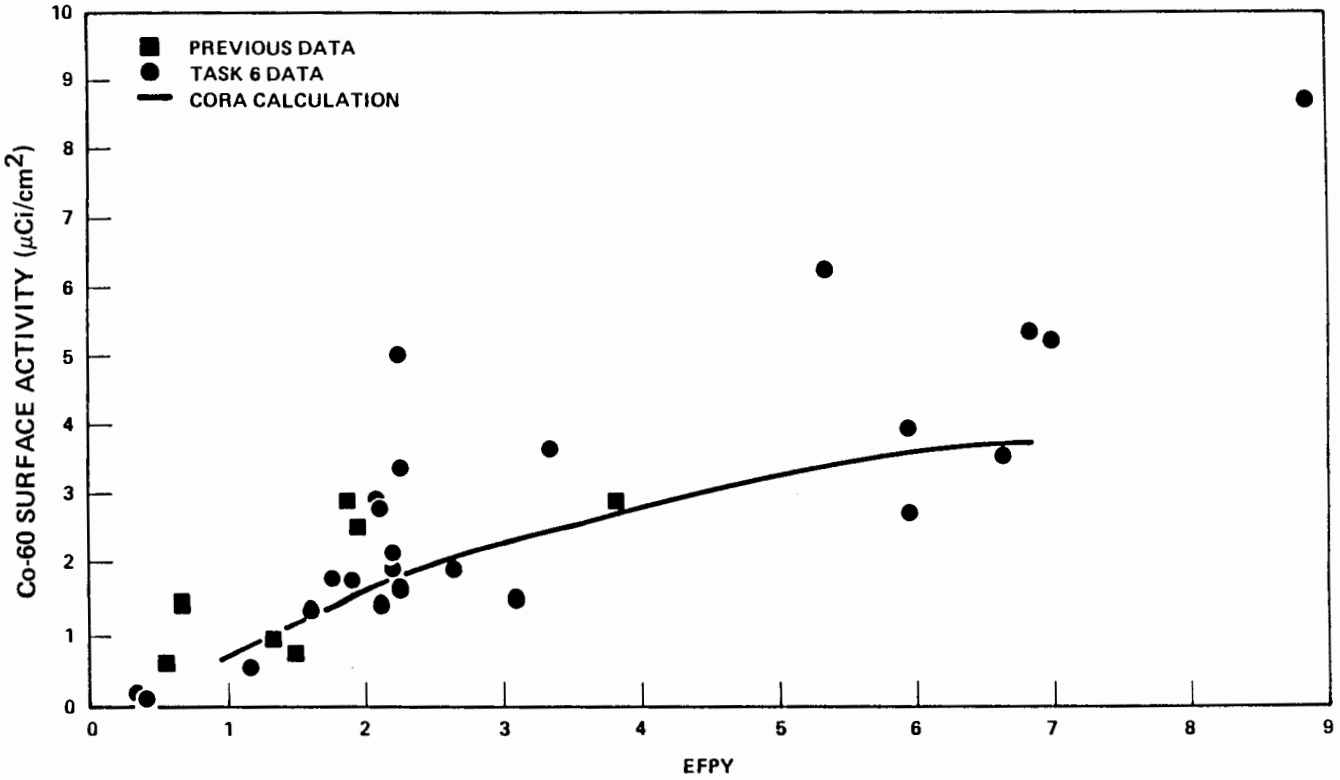

Figure 2-1. Steam Generator Tube Co-60 Surface Activity Versus EFPY

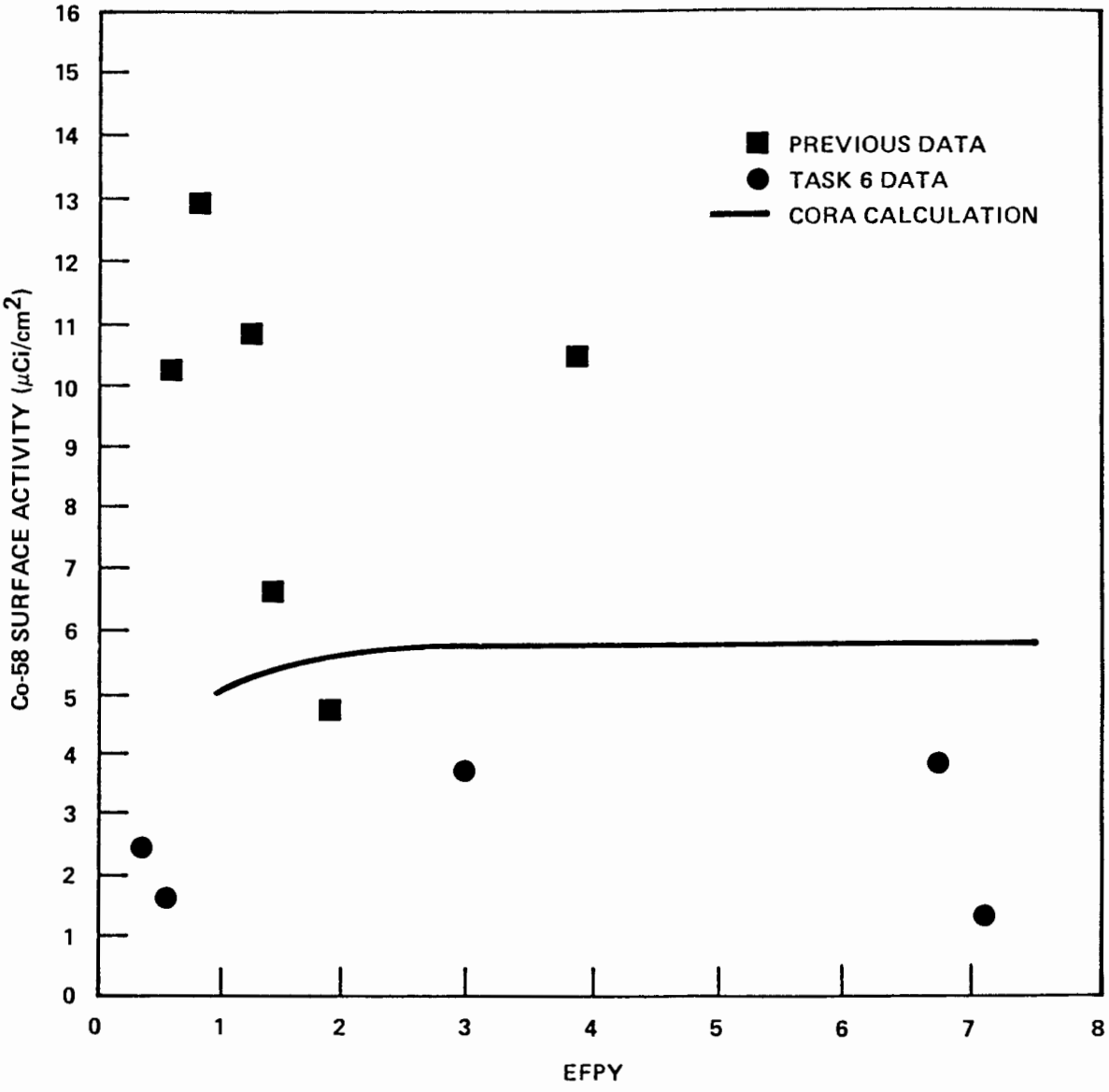

Figure 2-2. Steam Generator Tube Co-58 Surface Activity Versus EFPY

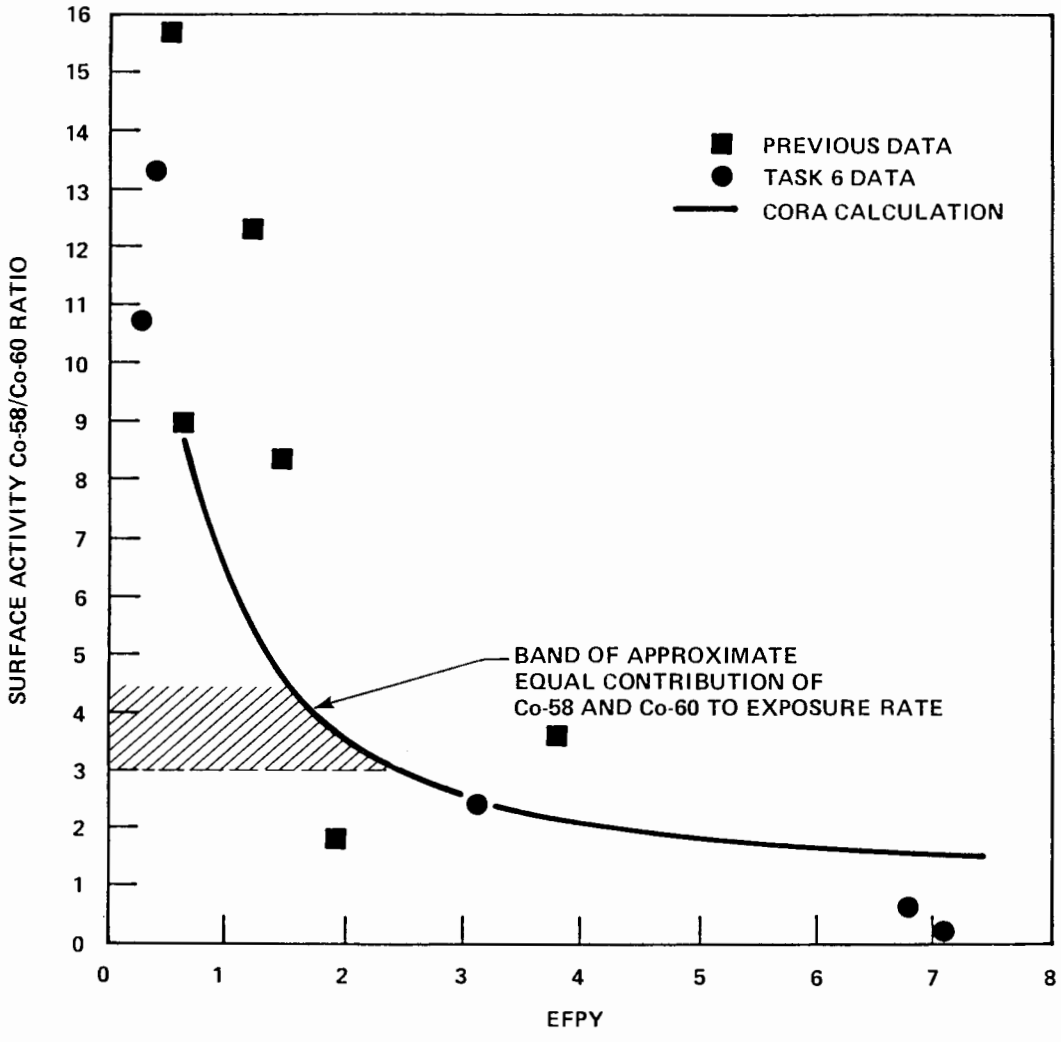

Figure 2-3. Steam Generator Tube Co-58/Co-60 Ratio Versus EFPY

summary can be given to facilitate discussion of the data. The CORA computer program incorporates the more fundamental aspects of transport, activation, and other crud-related mechanisms in a nuclear plant, and predicts several quantities of interest in addition to gross radiation level. CORA calculates the following out-of-core quantitites of interest as a function of time for the data available from this work: (1) activity and concentrations, (2) crud weight, and (3) crud specific activity. CORA utilizes eight nodes, as shown in Figure 2-4, for activity transport, plus two additional nodes (4 and 7) for mass transport. Node 4 represents the total mass of crud deposited on the core and node 7 represents the total mass out-of-core. For this report, the mechanisms occurring in nodes 6, 7, and 8 are of interest.

The general mass balance for a node can be expressed as follows:

Net Rate of Accumulation = Rate of Input - Rate of Loss

It is assumed that the transfer of a nuclide from one node to another is proportional to the mass of the nuclide in that node and the mass transfer coefficient for the transfer process between the nodes. Thus, the activity transfer rate between nodes can be calculated if the mass transfer coefficients can be determined.

As noted in Figure 2-4, out-of-core crud is divided into two arbitrary layers called transient and permanent. The net crud and activity buildup in the transient layer can take place by crud particle deposition from the coolant, erosion of the particle back into the coolant, transient-to-permanent crud transport, and soluble product transfer. The net crud and activity buildup in the permanent layer is determined by transient-to-permanent crud transport, and the molecular transfer between the solubles in the coolant and the permanent crud.

The particle deposition coefficients in CORA were calculated based on theory. The calculation of these coefficients depends strongly on particle sizes and flow regime. The circulating crud particle size is assumed to be 0.1 micron and the flow regime is assumed to be turbulent.

Since there is no good theory to estimate the erosion release coefficients, they were derived from the loop tests and plant data.

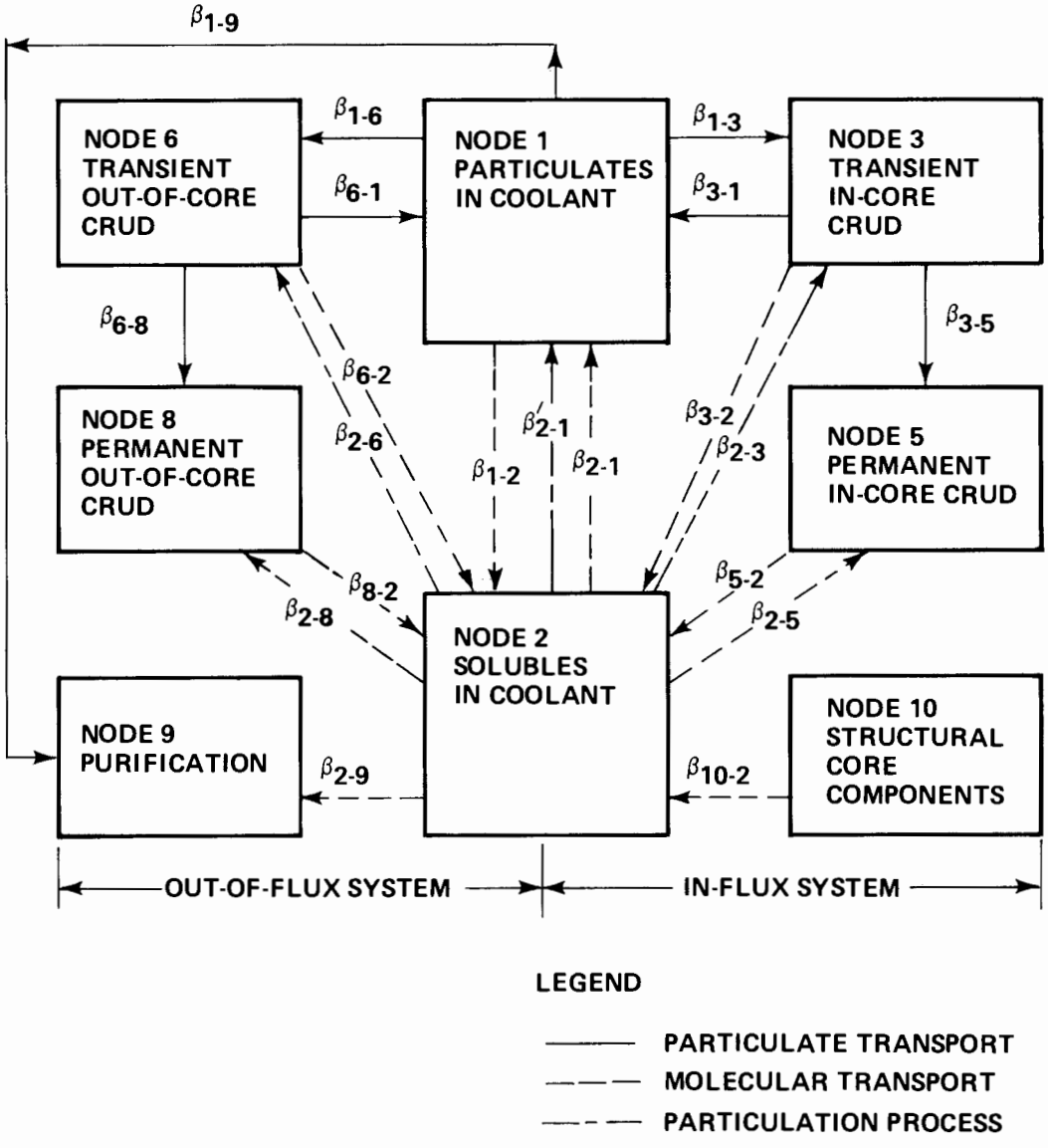

Figure 2-4. CORA Model Nodal Diagram

In CORA, soluble product particulation at the transient layer is the major mechanism through which new particles are formed. Some of the soluble product is partly removed by transfer directly to the permanent deposit. Since the generation rate from corrosion is greater than the effective deposition rate, the excess soluble products should go through a phase transformation by crystallization. Therefore, it is assumed that the excess corrosion products will be crystallized on the transient crud surface and thus provide new particles. The transient-to-permanent crud transport coefficient was determined based on diffusion mechanisms.

In the vicinity of any surface, the boundary layer coolant differs in composition from the bulk coolant in that it contains crud species contributed by the transient and permanent crud and, in the case of a tube corroding surface, the base metal itself. In CORA, the diffusion rate was divided into two terms, one involving the diffusion rate of active atoms out of the crud particles into the boundary layer coolant, and the other involving the diffusion through the boundary layer coolant to the permanent crud layer. The diffusion coefficients were determined based on theory and empirically based on plant data. The other coefficients involving the permanent layer are related to molecular and ionic transfer mechanisms between the solubles in the coolant and the permanent crud layer. These coefficients were determined based on theory and laboratory studies of corrosion product solubilities. In CORA, the long-term trend in radiation field buildup is accounted for by transfer mechanisms related to these coefficients.

Observations based on inspection of the data in Figures 2-1 through 2-3 include the following:

- The Co-60 trend is similar to that calculated by CORA except that the measured values appear to be about 50 percent greater than the calculated values.
- The Co-58 trend might be different compared to that calculated by CORA. The CORA-calculated value falls in the middle of the range of observed data; more Co-58 data are needed to establish a trend.
- The data trend of the Co-58/Co-60 ratio follows the CORA-calculated value. Note that after about 1.8 EFPY, Co-60 becomes the dominant contributor to the exposure rate.

It is also noted that most of the CORA-calculated Co-60 and Co-58 activities are in the transient layer compared to those in the permanent layer. However, since the definition of these layers is arbitrary, a comparison between the layers and the tube data is not meaningful; thus only the total CORA-calculated surface activity was chosen for comparison purposes.

COMPARISON OF STRAIGHT LENGTH AND U-BEND RADIOACTIVITY

A comparison was made between the activity on the straight length of tubing versus that on the small-radius U-bend tubing to define possible flow effects. Table 2-1 shows the comparison where data were available. There appears to be a trend toward more activity on the U-bends compared to that on the straight portions.

In Plant D, the Co-60 activity was higher on the U-bend than on the straight length even though the U-bend was of slightly fewer EFPY. In plant E, where both samplings were made at the same time, the activity on the U-bends was twice that on the straight portion. The U-bend deposit activity from Plant H was higher by a factor of three than that on the straight-length tube. However, from Figure 2-1, only a factor of two difference would be expected for the increased time of operation. Therefore, the trend appears to be that there is about twice as much activity on U-bends as on straight tubes. This indicates a possible effect of flow change on activity transport, because of a momentum change near the U-bend.

Table 2-1

COMPARISON BETWEEN ACTIVITY OBSERVED ON STRAIGHT AND U-BEND TUBING

Plant	Tube Type	EFPY	Average Co-60 Activity ($\mu Ci/cm^2$)	U-Bend to Straight Ratio
D	U-bend	2.09	2.87	1.4
	Straight	2.21	2.05	
E	U-bend	2.26	5.04	2.0
	Straight	2.26	2.50	
H	Straight	1.17	0.59	3.0
	U-bend	1.90	1.76	

RELATIONSHIP OF TUBING ACTIVITY AND CHANNEL HEAD EXPOSURE RATES

In a report of steam generator radiation level data, several anomalies were noted between twin plants and between steam generators within a plant (2). It was thought that examination of the steam generator tube activities and the exposure rates in the channel head might reveal explanations for the differences. A comparison of the steam generator tube activities with steam generator channel head exposure rates is provided in Table 2-2.

Table 2-2

STEAM GENERATOR CHANNEL HEAD EXPOSURE RATES AND TUBING ACTIVITIES

Plant	SG	EFPY	Co-60 Activity ($\mu Ci/cm^2$)	Average SG Channel Head Exposure Rate (R/hr)	Ratio of Exposure Rate To Activity
C	A	3.36	3.66	16	4.4
	B	5.35	6.24	9	1.4
D	B	2.21	1.93	8	4.1
	A	2.21	2.17	11	5.1
E	A	2.26	1.63	19	11.6
	C	2.26	3.39	20	5.9
F	A	6.64	3.58	19	5.3
G	A	5.96	3.94	8	2.0
	A	5.96	2.73	8	2.9
	A	6.84	5.38	9	1.7

One anomaly noted was that Plant E had average channel head exposure rates that were twice the exposure rates for Plant D at about the same EFPY. (Plants D and E are twin units built at the same time.) Similarly, the average channel head exposure rates in Plant F were twice the exposure rates in Plant G. (Plants F and G are also twin units.) However, the tube analyses reveal that the straight tubes in Plant E have on the average about 25 percent more activity than those in Plant D, and the activity on the tubes in Plant F is about the same as the average of activities in Plant G.

Another anomaly noted was that the channel head exposure rate in Plant C, steam generator A, was about twice the exposure rate in steam generator B. However, the activity on the tubes shows the opposite relationship: the tube activity in steam generator B is twice as high as that in steam generator A.

The above results suggest that there is something unique about the channel head exposure rates in one of each of the two twin plants that is not representative of the tubing activity. However, the exact reason is not known at this point. Likewise, the difference between the two steam generator exposure rates in the same plant and tubing activity is not defined by this comparison, but the data should contribute toward an evaluation of the anomalies.

In conclusion, there is not a good correlation between steam generator channel head exposure rates and the Co-60 activity on the tubing from the same steam generator.

Section 3

TUBING CRUD ANALYSES

SELECTION OF DESCALING TECHNIQUE

An evaluation of electrolytic and bromine-methanol descaling techniques was carried out on two adjacent tube sections from Plant D tube R5C40. Two 3-inch sections of the tube were cut. The outside surface of each section was sanded to bright metal and the sections were gamma counted. Each section was then mounted vertically in a dish using Paraplast cold setting resin. Each mounted tube section formed a small vertical container for the descaling solution or rinse water.

Electrolytic descaling was carried out by placing 15 milliliters of 0.1N nitric acid in the first tube section. A current of 0.5 amps at 1.0 volt was passed for 2 minutes between the tube section and a platinum cathode. The current causes the surface of the Inconel tubing to dissolve; thus the crud spalls off. After electrolysis, the electrolyte, along with the loose crud, was washed with demineralized water into a small beaker. The test section was then filled with water, treated ultrasonically, and washed again with water. Electrolyte and washings were filtered through a tared 0.45-micron, Type HA, Millipore filter.

Chemical descaling was achieved by treating the second tube section with 15 milliliters of a 1-percent bromine solution in methanol for 1 hour, followed by a 30-second ultrasonic treatment in demineralized water. Exactly like the electric current, the bromine-methanol solution causes the surface of the tubing to dissolve and the crud to spall off. The descaling solution and washings were combined and filtered through a tared 0.45-micron Gelman filter.

The efficiency of both descaling processes was monitored by measuring the fraction of Co-60 in the descaling solution and washings, and that remaining on the test section. The results of these preliminary experiments are listed in Table 3-1. It is seen that most of the material and activity is removed in the first descaling for either method. Likewise, nearly all of the activity removed was in the solids.

Table 3-1

COMPARISON OF ELECTROLYTIC AND CHEMICAL DESCALING

	Amount Removed			
	Electrolytic		Chemical	
Item	Co-60 (%)	Solids (mg)	Co-60 (%)	Solids (mg)
Solids in first run	91.2	6.07	86.8	5.26
Descaling solution from first run	1.1	--	0.5	--
Solids in second run	7.0	0.70	12.5	0.67
Descaling solution from second run	0.1	--	<0.1	--
Not removed from test section	0.6	--	0.1	--
Total in solids	98.2	6.77	99.3	5.93

In another experiment, the oxides removed from the inside of the steam generator tube sections were found to be virtually insoluble when subjected to either descaling technique. This indicated that the techniques did not solubilize the descaled material and thus the need to analyze the descaling solution was eliminated.

EDAX analyses of the material removed by both techniques indicated a similar elemental chemical composition. SEM scans of the underlying tubing surfaces showed that the bromine-methanol attacked the tubing surface more compared to the electrolytic method, as shown by comparison between Figures 3-1 and 3-2. The electrolytically descaled tubing surface shows definite grain boundaries, while the surface tested with bromine-methanol shows general attack with much less definition of grain boundaries.

Since the electrolytic descaling process was easier to control than the bromine-methanol method, the former was selected for this study. The descaled crud was dissolved in a mixture of aqua regia and hydrofluoric acid and the resultant solution was analyzed for chemical constituents by atomic absorption techniques.

Figure 3-1. SEM Image (1000X)* of Tube R5C40 Surface After Bromine-Methanol Descaling (2.21 EFPY)

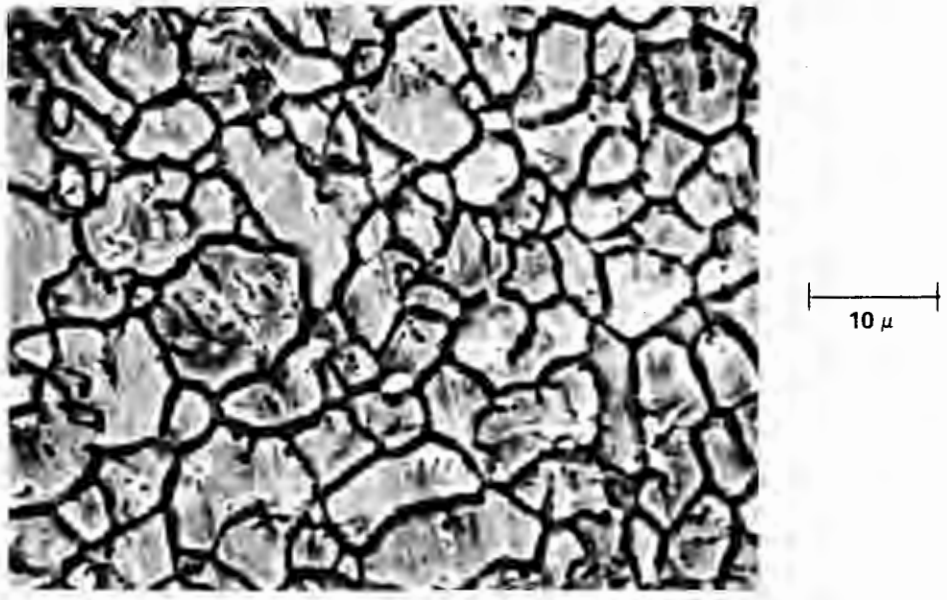

Figure 3-2. SEM Image (1000X)* of Tube R5C40 Surface After Electrolytic Descaling (2.21 EFPY)

*Please note that the illustration(s) on this page has been reduced 10% in printing.

WEIGHT AND SURFACE CONCENTRATION OF CRUD

Six steam generator tube sections with exposures between 1.6 and 7.0 EFPY were descaled electrolytically. The areas descaled, weights of crud, surface concentrations, actual thickness measured on SEM images, and a computed crud density are listed in Table 3-2.

Table 3-2

DATA ON CRUD REMOVED FROM SELECTED STEAM GENERATOR TUBES

Plant	EFPY	Area Descaled (cm^2)	Weight of Crud (mg)	Surface Concentration (mg/dm^2)	Film Thickness (microns)	Apparent Density (gm/cm^3)
E	1.58	34.05	3.88	11.4	N/D[a]	N/D
B	1.75	31.71	4.04	12.7	N/D	N/D
D	2.21	31.47	6.07 6.77[b] 7.38[c]	19.3 21.5[b] 23.4[c]	N/D	N/D
G	5.96	32.25	15.44 18.43[b] 19.15[c]	47.9 57.1[b] 59.4[c]	1.20	3.99 4.76[b] 4.95[c]
G	6.84	35.88	11.94 12.61[b]	33.3 35.1[b]	0.85	3.92 4.13[b]
A	7.02	31.89	13.86 23.39[b]	43.5 73.3[b]	1.14	3.81 6.43[b]

[a]Not determined
[b]Includes a second descaling
[c]Includes a third descaling

For four of the tubes, data from the second or third descalings were included since the chemical analyses (see Table 3-3) suggested that the material removed was still representative of the crud as opposed to that of the tubing. The data are plotted in Figure 3-3 as a function of EFPY. A least-squares fit of the surface concentrations with operating time using the total weights obtained by descalings indicated that the surface concentration increased by about 8.3 mg/dm^2 per EFPY.

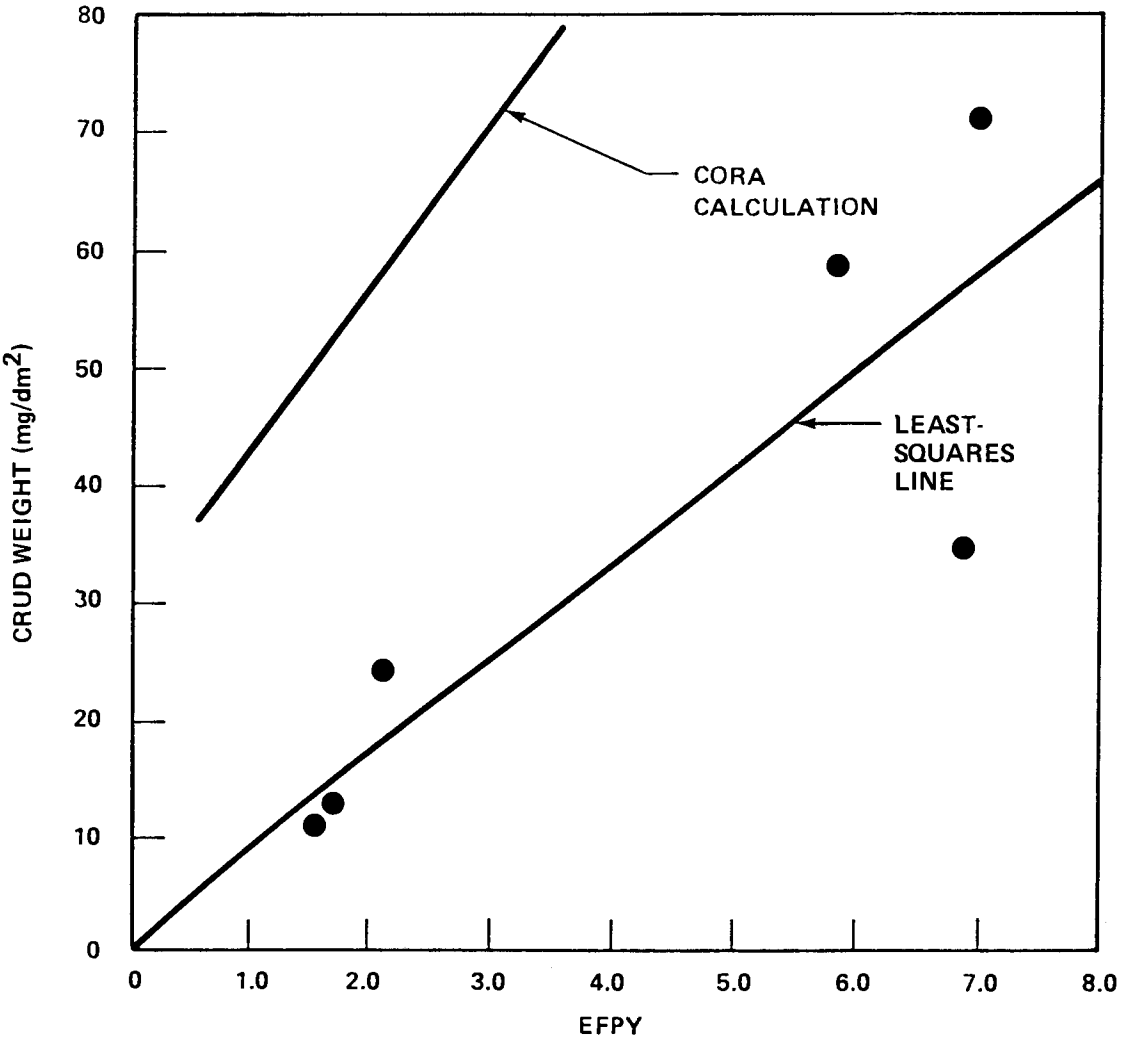

Figure 3-3. Crud Weight Versus EFPY

Also shown on Figure 3-3 is the crud surface concentration calculated by CORA for a plant operated with the type of chemistry control typical of those in the sampling program. The surface concentration calculated by CORA is about three times that observed and represents only permanent material. Since, in general, the tubing samples had been forcefully removed from plants and had been transported and handled, the film removed should be more representative of permanent deposits. Visual inspection of the tubes indicated that most of the material descaled (more than 95 percent) would be considered permanent since little activity was in the transport containers or came off the tubes when they were handled.

The 8.5 mg/dm^2 per EFPY slope is equivalent to 0.71 mg/dm^2-mo of crud or 0.5 mg/dm^2-mo of metal. This 0.5 value represents the difference between the corrosion rate and corrosion release rate of the Inconel tubing assuming that crud deposition is negligible. Using a nominal value of 3 mg/dm^2-mo for the corrosion rate of Inconel (3), a corrosion release rate of 2.5 mg/dm^2-mo is estimated. This compares favorably with that of 1.5 mg/dm^2-mo used in other work (1).

CHEMICAL COMPOSITION OF CRUD

Table 3-3 gives the amount of material descaled and its chemical composition by fraction descaled, where chemical composition is for the oxide form.

Inspection of the data shows that for each successive descaling, the composition of the removed material approaches that of the Inconel base metal, that is, about 8 percent iron, 74 percent nickel, and 18 percent chromium. This indicates that a substantial portion of the material being removed is representative of the base metal.

The chemical concentrations of nickel and chromium in the first descaling appear to vary as a function of exposure, as shown in Figure 3-4. Using the method of least squares, the percentage of nickel increases with time, the percentage of chromium decreases with time, and the percentage of iron stays about the same. Although not plotted, the percentage of cobalt is shown by the data to also stay about the same. It is also noted that iron, chromium, and cobalt are enriched and nickel is depleted in the descaled material compared to the base metal. As shown in Table 3-4, the percentage of the elements in the first descaling was found to be very similar to that found by EDAX analyses of the surface layer of the material in the tube before descaling.

Table 3-3

CHEMICAL COMPOSITION OF MATERIAL DESCALED FROM TUBES

Plant	EFPY	Descaling Sequence	mg/cm^2 Descaled	Percentage of Element in Descaled Material[a]					Percent Cobalt in Tubing	Percent Cobalt in Tubing if Oxide
				Fe	Ni	Cr	Mn	Co		
E	1.58	1	0.11	14.0	19.7	37.6	0.16	0.28	0.039	0.027
		2	0.03	10.6	45.1	18.8	0.19	0.09		
		3	0.02	7.8	48.8	18.3	0.19	<0.08		
B	1.75	1	0.13	14.5	20.5	35.9	0.65	0.22	0.020	0.014
		2	0.03	9.2	49.9	16.1	0.22	<0.08		
		3	0.03	9.2	51.1	15.0	0.14	<0.08		
D	2.21	1	0.19	21.6	26.8	24.2	0.21	0.26	0.048	0.034
		2	0.02	20.5	31.7	19.8	<0.30	N/D[b]		
		3	0.02	17.3	37.4	17.3	<0.30	N/D		
G	5.96	1	0.48	20.4	30.1	22.6	0.20	0.12	0.021	0.015
		2	0.09	15.7	32.7	24.8	0.22	0.09		
		3	0.02	15.8	26.6	29.9	0.34	<0.08		
G	6.84	1	0.33	20.0	23.1	26.9	0.31	0.20	0.039	0.027
		2	0.02	18.2	30.4	23.4	<0.30	0.22		
		3	0.01	10.2	43.0	18.8	<0.30	0.09		
A	7.02	1	0.44	14.8	39.0	20.0	0.22	0.36	0.038	0.027
		2	0.30	15.9	38.2	17.5	<0.30	0.14		
		3	0.15	8.9	50.4	12.7	<0.30	0.04		

[a]Estimated standard deviation of analysis error:
Fe, Ni, Cr = 3%
Mn = 5%
Co = 10%
[b]Not determined

The percentages of iron and chromium in the descaled material generally decrease with each descaling and approach that of the base tubing. The percentage of cobalt in the descaled material generally decreases with each descaling but is greater than that in the base tubing. An estimate was made of the total amount of cobalt on the steam generator tubing surface as represented by the first descaling. It was found that this amount was about 45 grams, regardless of the time of plant operation. If the time of plant operation is taken into account, about 25 grams per year was on the earlier tubes (about 2 EFPY) and about 7 grams per year on the later tubes (about 6.5 EFPY). The value of 25 grams in early operation is somewhat less than that of 60 calculated in a recent cobalt source study (4). The decreasing value with time suggests a decreasing cobalt input rate with time.

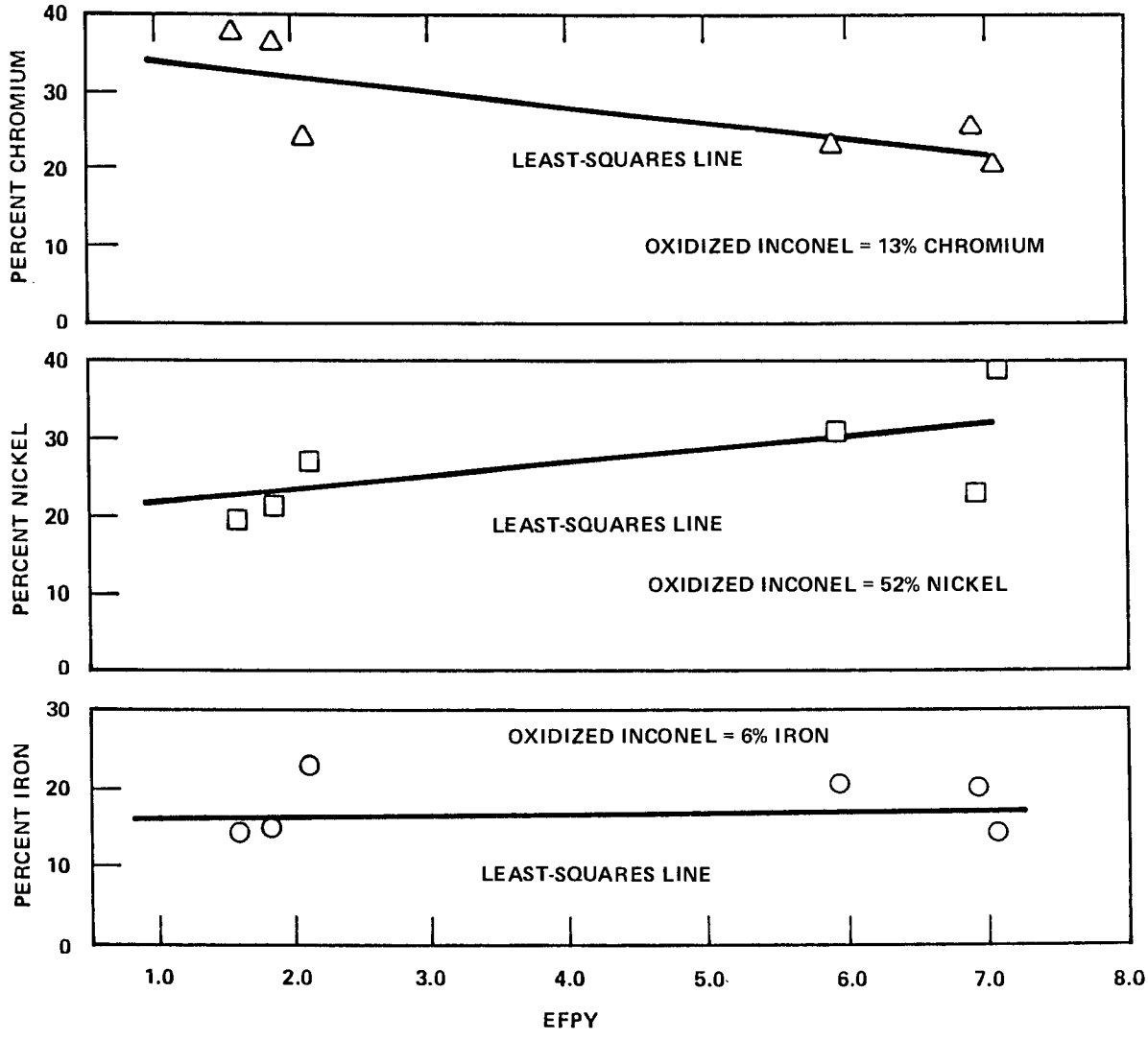

Figure 3-4. Variation of Elemental Percentages in Descaled Material With EFPY

Table 3-4

COMPOSITION OF CRUD ON TUBE SURFACE BY EDAX OR ATOMIC ABSORPTION AND COMPARISON WITH THAT REMOVED IN FIRST DESCALING

Plant	EFPY	Tube	Relative Percentage of Indicated Element[a] Chromium	Nickel	Iron
B	1.76	R1C25	33	40	27
G	5.96	R18C37	35	43	22
G	6.84	R15C73	43	36	21
A	7.02	R36C37	33	39	28
Average percentage by EDAX in total crud			36	40	25
Average percentage by EDAX of element assuming 30% is oxide			25	28	18
Average percentage by atomic absorption of element removed in first descaling			26	27	18

[a] The three elements listed constitute essentially all the elements in the crud.

The relationship of the percentage of cobalt in the tubing to that in the first descaled material is shown in Figure 3-5. The physical meaning of the apparent direct relationship is not known at present.

The nickel-to-iron ratio in the steam generator tube deposits ranges from 1.2 to 2.6, compared to 9.2 in the base metal. Typical core deposits have ratios between 0.3 and 0.7. The high nickel-to-iron ratio indicates that either metallic nickel or NiO occurs in the tube deposits, besides nickel ferrite. The chromium concentration in the tube deposits is appreciably higher than in core deposits, ranging from 20 to 38 weight percent; typical core deposits have chromium concentrations between 1 and 8 weight percent.

Crud samples from tubes from Plant A (tube R36C37) and from Plant G (tubes R18C37 and R15C73) were analyzed by X-ray diffraction using the Debye-Scherrer powder method, in which the diffraction lines were recorded on a strip of photographic film. In the Debye-Scherrer method, X-rays of a known wavelength are used to

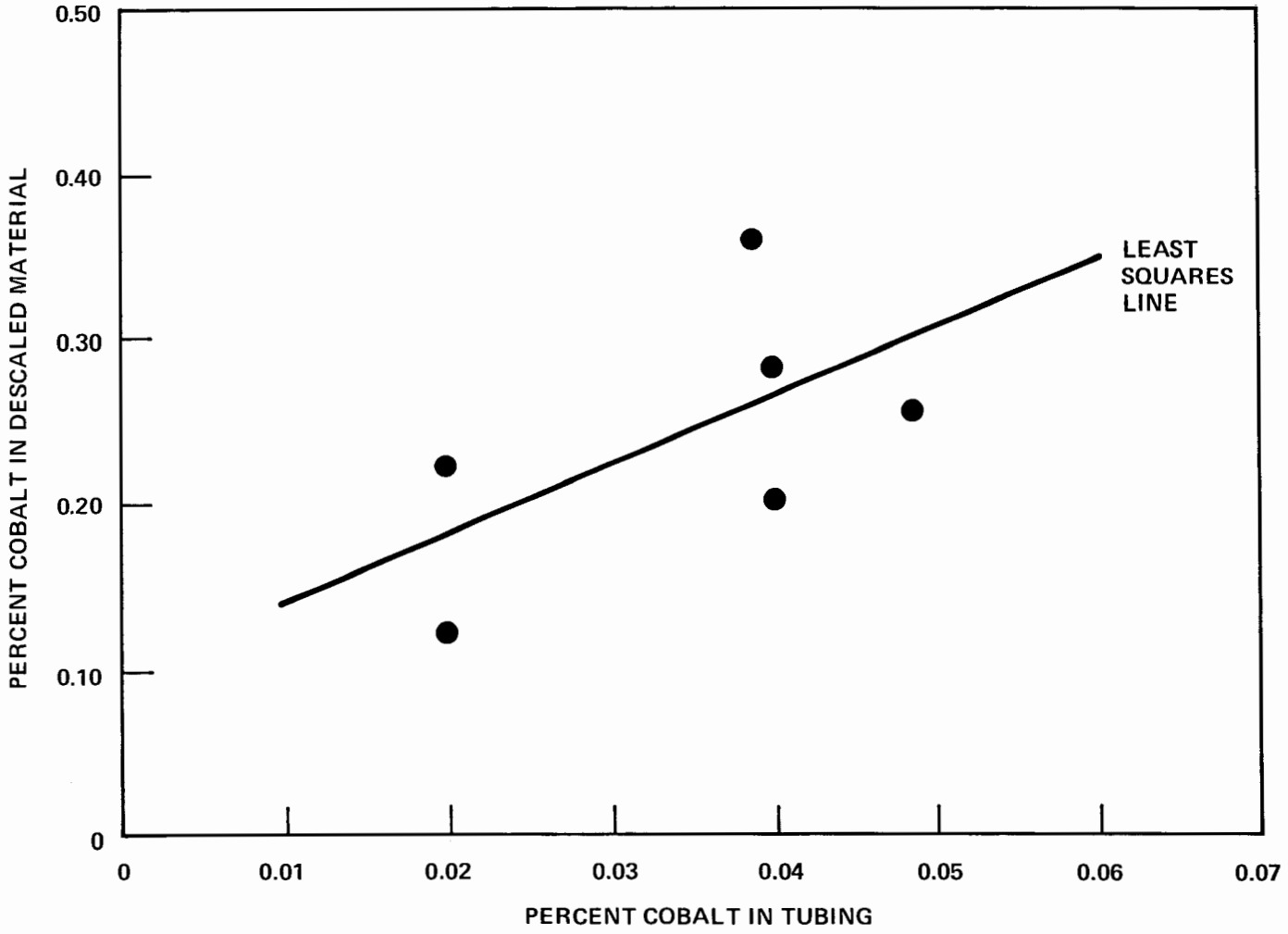

Figure 3-5. Percentage of Cobalt in Descaled Material Versus Percentage of Cobalt in Steam Generator Tubing

determine the unknown spacing of planes in the crystal lattices of sample crystallites. The patterns obtained differed only in line intensities and matched the standard patterns of metallic nickel and of the spinels nickel ferrite ($NiFe_2O_4$) and nickel chromite ($NiCr_2O_4$).

The question whether crud from the above steam generator tubes, whose major constituents are Ni, Cr, and Fe, contain two separate spinel phases besides metallic nickel, usually nickel ferrite and nickel chromite, was further investigated by a variation of the Debye-Scherrer method, using a diffractometer. This instrument uses a Geiger-Müller (G-M) X-ray detector tube instead of a photographic film to record angle and intensity of diffraction lines. Also, the G-M detector scans the sample holder at a preset rate during irradiation with monochromatic X-rays. The slower the scan rate, the higher the angular resolution of adjacent diffraction lines.

Crud samples from steam generator tubes from the above plants (A and G) were analyzed on a diffractometer at its lowest possible scan rate, 0.8 degrees per minute. The intensity-versus-angle diagrams obtained did not resolve lines, suspected to be generated by superposition of closely spaced lines from the above spinels. This observation suggests that very likely only one spinel phase was present in the samples.

If this spinel were nickel ferrite, then the spacings derived from diffractometer and powder patterns should yield a reasonable lattice parameter, somewhere between 8.33 and 8.39 Å depending on the x in $Ni_xFe_{3-x}O_4$. An evaluation of the above spacings led to lattice parameters well outside these limits. Apparently, the spinel phase in the above samples is not a simple ferrite but probably a mixed ferrite or chromite with the composition $Ni_xCr_yM_zFe_{3-x-y-z}O_4$ (ferrite) or $Ni_xFe_yM_zCr_{3-x-y-z}O_4$ (chromite), where M represents small concentrations (less than 1 percent) of Co and/or Mn. It is quite possible that the values x, y, and z are not constant in deposits taken from different elevations on a given tube or from different tubes.

Since ferrites, even mixed ferrites which contain an unknown minimum concentration of Fe (5), are ferromagnetic and chromites are not, thermomagnetic analysis of the above tube crud samples would offer a possibility of determining whether the mixed spinel phase in these crud samples is a ferrite or a chromite. Thermomagnetic analysis has the objective of determining the Curie point of a ferromagnetic substance. The Curie point is the temperature at which its ferromagnetism disappears. The small quantity (a few micrograms) of crud sample material available

was insufficient for an accurate thermomagnetic analysis; typical sample weights required range from 5 to 10 milligrams. Still, the following simple tests were carried out.

A suspension of tube crud samples in water in a test tube and, for comparison, an equal quantity of magnetite in water in a second test tube, were exposed to a strong magnetic field. The tube crud sample contained two distinct fractions. The smaller fraction was attracted mildly to the magnet. This material is believed to be nickel. The major portion of the tube crud did not react at all to the magnet. By contrast, magnetite was very strongly attracted. The behavior of the major portion of the crud samples suggests that this material is probably a mixed chromite. The possibility that the above materials are ferrites whose iron concentration is below the level necessary to make them ferromagnetic is believed to be quite low because the chromium concentration in these materials is greater than the iron concentration.

The X-ray diffraction patterns obtained on a film strip by the Debye-Scherrer powder method also include lines resulting from large angle reflections ("back reflection"). (Large here refers to angles between incident and reflected beam of more than 90 degrees.) The intensity of such back reflections is a function of crystallite size. The smaller the individual crystallites, the less X-rays interact with them. The back reflections in the powder diagrams from the above crud samples were very faint, suggesting that the average diameter of the crystallites in the samples was of the order of 0.1 micron.

RADIOCHEMICAL COMPOSITION OF CRUD

The radiochemical composition of crud removed from selected steam generator tubes is listed in Table 3-5 in $\mu Ci/cm^2$, $\mu Ci/mg$ crud, and $\mu Ci/mg$ parent. The values are based on the material and activity removed by the first descaling only.

Based on the data in Table 3-5, the Co-60 activity per unit area increases by about 0.7 $\mu Ci/cm^2$ per EFPY. The Mn-54 activity seems to decrease with EFPY while that of Fe-55 seems to increase slightly. A decrease in activity for all nuclides in terms of $\mu Ci/mg$ of crud and $\mu Ci/mg$ of parent is apparent. The specific activities in $\mu Ci/mg$ of crud for Mn-54, Fe-55, and Co-60 are plotted in Figure 3-6 along with the values calculated by CORA. It is seen that for Co-60, the observed decreasing trend matches that calculated by CORA except that the values are greater by a factor of about four. However, there are few data points and those after 6 EFPY have considerable scatter. Previously it was noted that the crud

Table 3-5

ACTIVITY OF CRUD ON STEAM GENERATOR TUBES CORRECTED TO SHUTDOWN

		Activity[a] in $\mu Ci/cm^2$			
Plant	EFPY	Fe-55	Mn-54	Co-58	Co-60
E	1.58	0.45	--	--	1.44
B	1.75	0.65	0.27	--	1.72
D	2.21	1.02	--	--	2.24
G	5.96	2.46	0.28	--	3.99
G	6.84	1.34	0.15	3.98	5.22
A	7.02	0.90	0.08	1.16	5.86

		Activity in $\mu Ci/mg$ Crud			
Plant	EFPY	Fe-55	Mn-54	Co-58	Co-60
E	1.58	3.95	--	--	11.4
B	1.75	5.11	1.88	--	12.0
D	2.21	5.29	--	--	10.8
G	5.96	5.14	0.51	--	7.1
G	6.84	4.03	0.43	11.5	15.2
A	7.02	2.07	0.12	1.7	8.9

		Activity in $\mu Ci/mg$ Parent			
Plant	EFPY	Fe-55	Mn-54	Co-58	Co-60
E	1.58	28	--	--	4100
B	1.75	35	13.0	--	5500
D	2.21	24	--	--	4200
G	5.96	25	2.5	--	5900
G	6.84	20	2.2	50	7600
A	7.02	14	0.8	4	2500

[a]Properties of Nuclides:

Nuclide	Parent	$t_{1/2}$	Major Gamma Energy
Co-60	Co-59	5.3 yr	1.13, 1.17
Fe-55	Fe-54	2.7 yr	None
Mn-54	Fe-54	312 days	0.84
Co-58	Ni-58	71 days	0.81

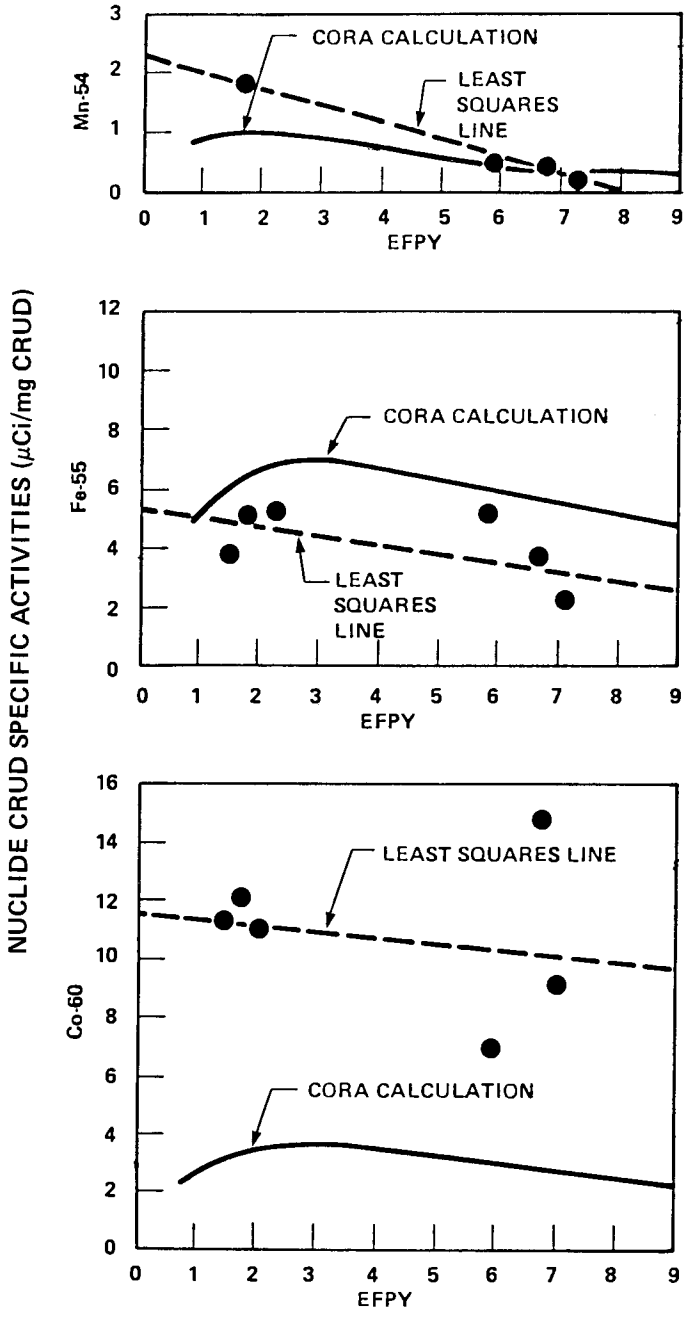

Figure 3-6. Nuclide Crud Specific Activities Versus EFPY

weight calculated by CORA was greater by a factor of three than that observed. Thus, if the weight were adjusted downward, the CORA values and observed Co-60 values would more nearly match. The lower CORA value can also be due to the lower percentage cobalt in crud assumed in CORA (about 0.1 percent), compared to that observed in tube crud (about 0.3 percent). The CORA-calculated Mn-54 values appear to match the observed data fairly well; the CORA-calculated Fe-55 values are about one and one-half times those observed. However, if the values were adjusted for a better matched crud weight, the CORA values would be considerably greater than those observed. For both nuclides, the trend of the data also matches that calculated by CORA.

The data in Table 3-5 are based on that material removed in the first descaling only. Similar data for subsequent descalings, where available, are given in Table A-4. Inspection of these data reveals that the crud specific activity for Co-60, Mn-54, and Co-58 decreases with each descaling. For Mn-54 and Co-58, a similar decrease with each descaling is noted in term of specific activity per mg of parent. In addition, for Mn-54, a decrease with EFPY is seen, as shown in Figure 3-7. A similar decrease for Co-60 is not evident. These differences in activity behavior between nuclides are probably due to differences in their half-lives.

PHYSICAL CHARACTERIZATION OF CRUD

Before removal of the material from the four steam generator tube sections selected for physical analysis, contact autoradiographs were made with standard 35mm film. The autoradiographs of the tubes from Plants A and G showed a relatively even distribution of activity on the inside surfaces. The autoradiograph of the crud on the tube section from Plant B (tube R1C25) is shown, slightly magnified, in Figure 3-8. Over a fine-grained dark background are a few "hot spots." EDAX analysis of a dark area near the center of this tube section indicated that iron, nickel, and chromium are the major elements in the material. This particular EDAX spectrum is reproduced in Figure 3-9.

SEM images of three of the hot spots in the crud on the steam generator tube from Plant B are shown in Figure 3-10. EDAX analysis of these hot spots was virtually identical with that of the dark area. This indicates that the spots are transparent to X-rays and that the atomic numbers of the constituent elements of the hot spots must be less than 10. In addition, the white coloration of the spots, caused by fluorescence, is another indication that the atomic numbers of the constituent elements are less than 10. The white material of the spots is believed to be boric acid. (The EDAX equipment is not capable of detecting

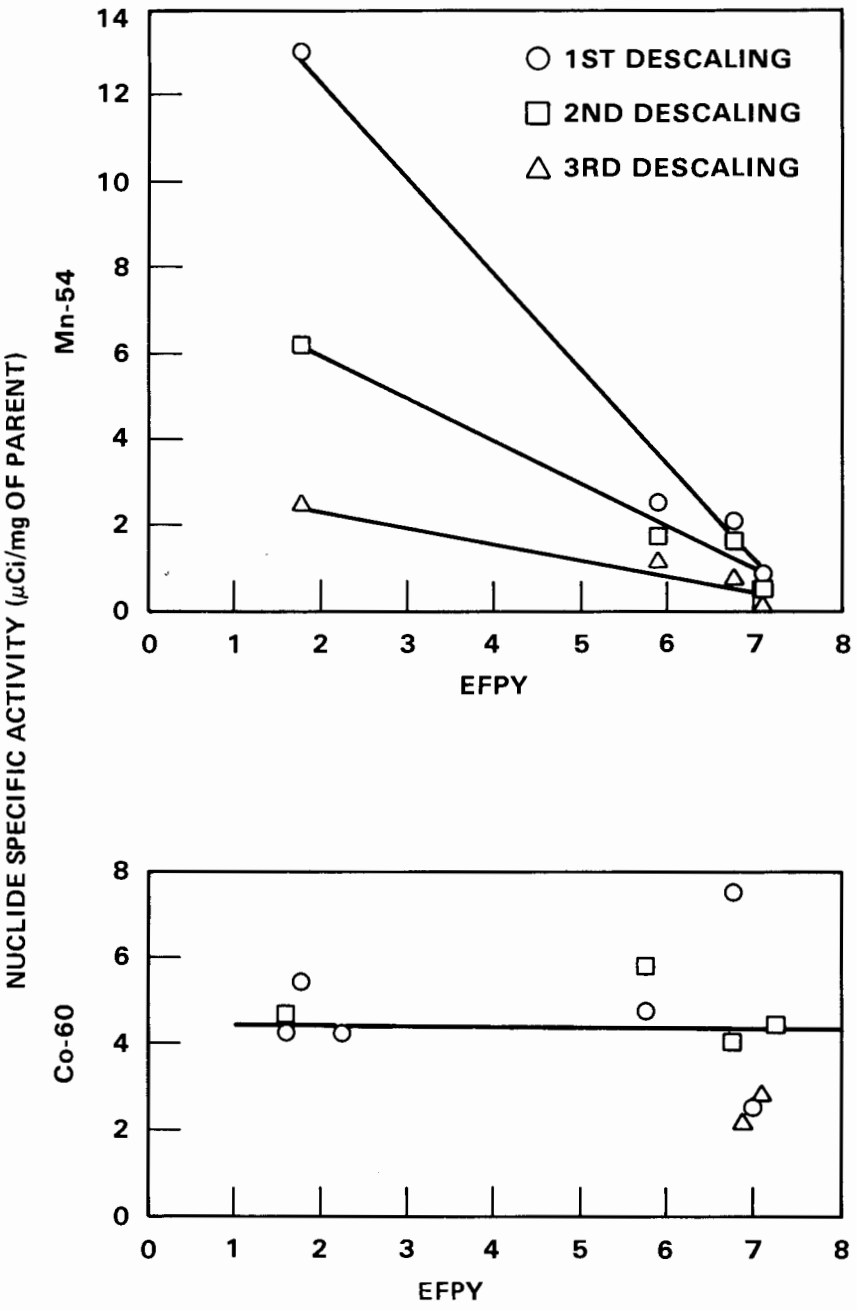

Figure 3-7. Nuclide Specific Activity Variation With Descaling Fraction and EFPY

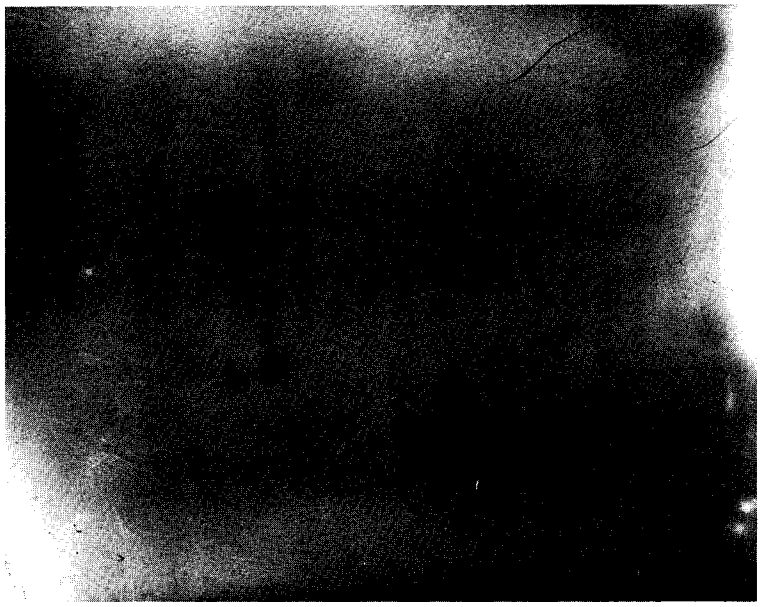

Figure 3-8. Autoradiograph of Tube R1C25 Showing Hot Spots

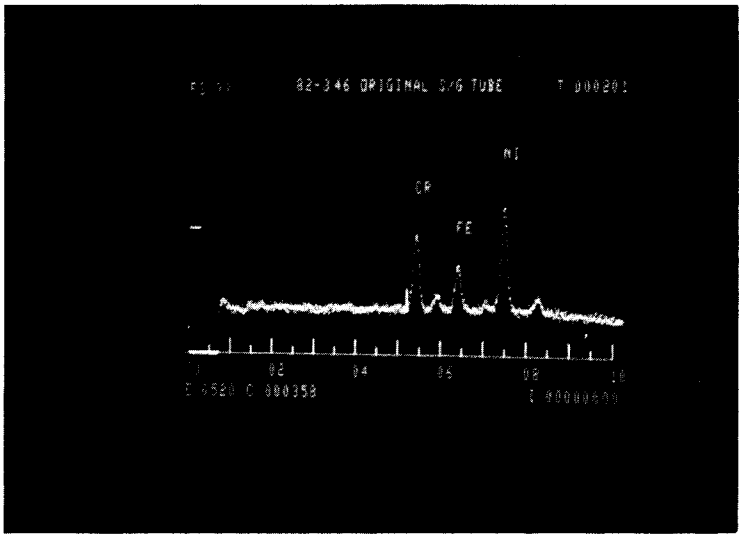

Figure 3-9. EDAX Analysis of Central Dark Section of Tube RC125

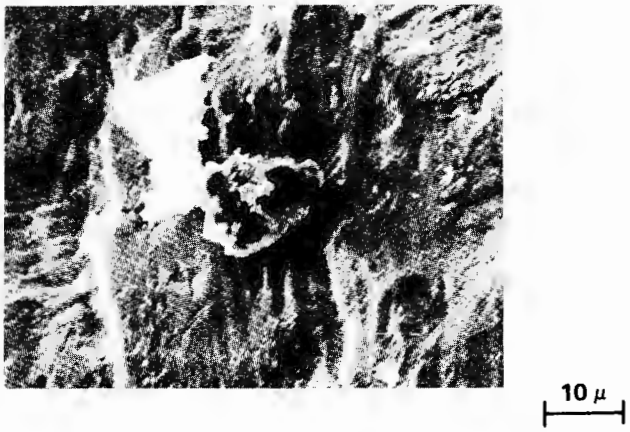

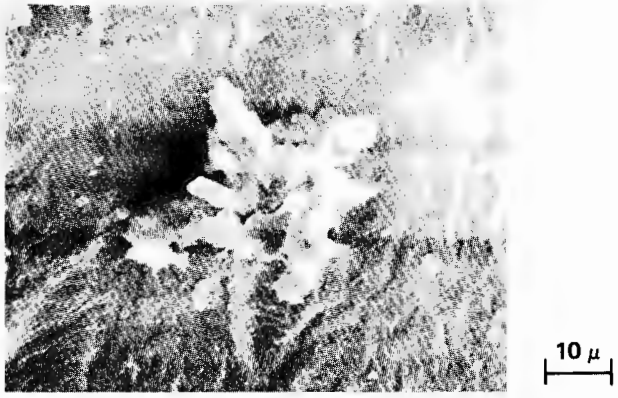

Figure 3-10. Various Hot Spots in Crud on Tube R1C25

elements whose atomic number is less than 10.) The greater activity of the hot spots could be caused by increased concentration of coolant activity due to the concentration of boric acid crystals.

The crud on the tube section from Plant B (R1C25), shown in Figure 3-11 at 1000X, consists of very small crystallites that appear to give a smooth surface, even at high magnification. The surface of this material shows narrow cracks that form irregularly shaped agglomerates of crystallites. A similar pattern of cracks has been noted in other work (6) and is believed to represent grain boundaries. The white, approximately spherical crystals are presumed to be boric acid.

The cystallites in the crud on the Plant A tube section (R36C37) were also so small that they were not resolved by the SEM at 1000X, as shown in Figure 3-12. However, the material cracks appear to be wider than those in Plant B and again appear to follow the presumed grain boundaries. An appreciable quantity of dark, needle-shaped crystals and irregularly shaped white crystal aggregates also appears embedded in the crud. The needle-shaped crystals were found to contain phosphorus (probably as phosphate) at a surface concentration of 5 $\mu g/cm^2$. Similar to Plant B, the white crystal aggregates are believed to be boric acid.

SEM images at 1000X of the crud on the two tube sections from Plant G are shown in Figures 3-13 and 3-14. The crystallites of the material on both tubes again are so small that they were not resolved by the SEM. The crud on tube R15C73 shows a pattern of wide, generally parallel cracks; the crud on tube R18C37 exhibits parallel ridges with fairly wide cracks at right angles to the ridges. The wide cracks in the material on Plant G and Plant A steam generator tubes could reflect the longer time of exposure compared to that of Plant B.

Comparison of the undescaled tubing surfaces in Figures 3-11 through 3-14 with that of the descaled tubing surface in Figure 3-2 shows a similar pattern, although the sizes of the boundaries on the undescaled tubing appear to be somewhat greater than those on the descaled surface, indicating a layer of crud on the tubing surface. An SEM image of the material removed by the electrolytic descaling process is shown in Figures 3-15. The materal appears to be flake-like; the sizes vary from about 30 microns down to several microns.

SEM images were also made on cold mounted and polished sections of tubing for direct measurement of the crud thickness, which permitted the calculation of the apparent density of the respective crud. Images of the tube wall and crud layer

Figure 3-11. SEM Image of Crud From Tube R1C25 at 1000X*(1.75 EFPY)

Figure 3-12. SEM Image of Crud From Tube R36C37 at 1000X*(7.02 EFPY)

*Please note that the illustration(s) on this page has been reduced 10% in printing.

Figure 3-13. SEM Image of Crud From Tube R15C73 at 1000X*(6.84 EFPY)

Figure 3-14. SEM Image of Crud From Tube R18C37 at 1000X*(5.96 EFPY)

*Please note that the illustration(s) on this page has been reduced 10% in printing.

Figure 3-15. SEM Image (1000X)* of Crud Removed From Tube R5C40 Using Electrolytic Descaling Technique (2.21 EFPY)

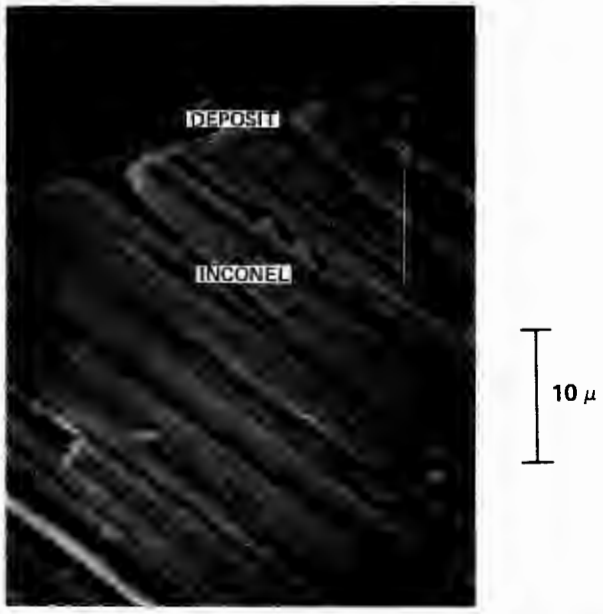

Figure 3-16. Tube Wall and Crud Layer of a Plant G Tube Section

*Please note that the illustration(s) on this page have been reduced 10% in printing.

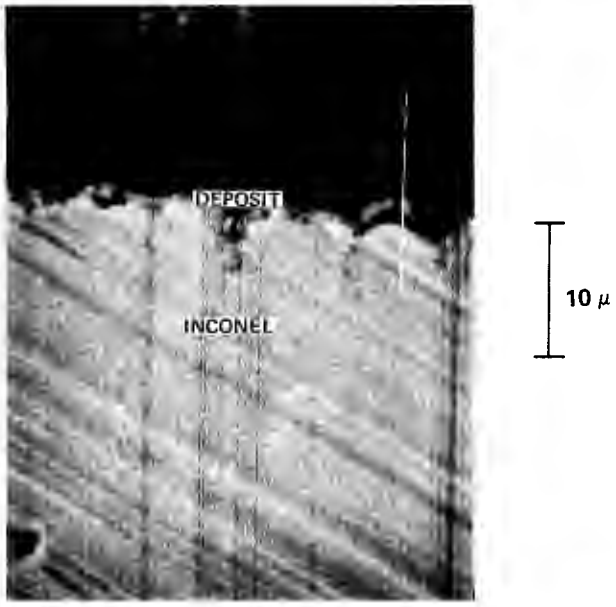

Figure 3-17. Tube Wall and Crud Layer of Another Plant G Tube Section

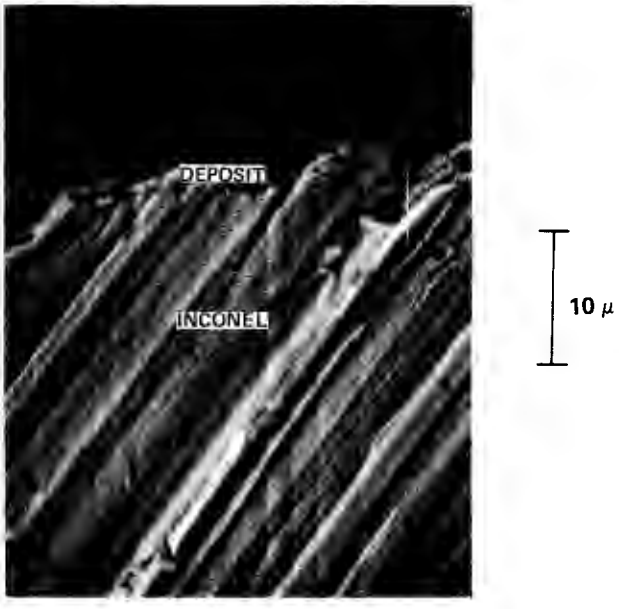

Figure 3-18. Tube Wall and Crud Layer of a Plant A Tube Section

of the two Plant G tube sections and of the tube section from Plant A, taken at zero degrees tilt, are shown in Figures 3-16, 3-17, and 3-18. The thicknesses of crud measured by this approach, listed in Table 3-2, averaged about 1 micron. The average apparent density of 3.9 g/cm^3 is about 70 percent of the theoretical density of magnetite, or about 40 percent of that of metallic nickel. The finger-like extensions of the crud in the tubing were also noted in the previous work (6).

COMPARISON OF TUBE AND CORE CRUD

A comparison of the physical characteristics of the crud on steam generator tubes with those of core crud, as presented in Table 3-6, shows clearly that the composition of steam generator tube crud is closer to the composition of the corroding matrix material, Inconel-600, than that of core crud. This indicates that most of the tube crud originates from the corrosion of the base metal.

The major difference in the radiochemical composition (in $\mu Ci/mg$ of parent) of tube crud and core crud is a much larger specific activity of core crud than tube crud. The fact that the steam generator tube deposit is radioactive proves that there is interaction with the reactor coolant and that there is transport of dissolved or solid species from the tube to the core and back.

Crystallographic analyses of crud samples on steam generator tubes established the presence of metallic nickel. Indirect evidence was obtained that a second major phase in the above crud sample is a spinel, very likely a complex chromite. To determine unambiguously the detailed composition of the complex chromite, such tools as Mössbauer spectroscopy, thermomagnetic analysis, and X-ray diffraction analysis must be employed, both on larger (10-25 mg) crud samples and on synthetic chromites of a variety of compositions.

The greater density of the crud on steam generator tubes compared with core crud is consistent with the suggestion that the major fraction of the tube material was formed *in situ* by corrosion and the minor portion by deposition from the coolant.

Information on the size of individual crystallites in the crud on steam generator tubes could not be extracted from SEM images since images at 1000X did not resolve individual crystallites. This observation suggests that the crystallites have dimensions of less than 1 micron. The X-ray diffraction analyses did not yield any supplemental information on the size of individual crystallites in the tube deposits.

Table 3-6

COMPARISON OF CHARACTERISTICS OF TUBE CRUD AND CORE CRUD

Item	Steam Generator Deposit	Core Deposit[a]	Oxidized Nominal Tube Material
Chemical composition (%)			
Fe	14-22	39-47	6
Ni	20-30	19-24	52
Cr	20-38	0.8-2.5	13
Co	0.24	0.11	0.035
Radiochemical composition (μCi/mg parent)			
Co-58	4-50	800-1300	
Co-60	2500-6000	25,000-100,000	
Crystallography			
$Ni_xFe_{3-x}O_4$	Probably not present	$0.4 < X < 0.9$	
Mixed Fe,Cr spinel	Present	Not detected	
NiO	Not detected	Sometimes present	
Ni	Present		
Surface concentration (mg/dm^2)	11-60	10-350	
Density (gm/cm^3)	$\sim$ 4	1.2 (estimated)	

[a] Plant B, cycle 1 and 2 typical data

Section 4

SUMMARY AND CONCLUSIONS

As a result of the work performed for this report, the following can be summarized and concluded regarding material removed from steam generator tubes in Westinghouse-designed nuclear plants:

- The standard deviation of the average activity along the straight length of tubing of the same tube from above the tubesheet to the U-bends was found to be within ±20 percent. Similarly, the standard deviation between different tubes in the same steam generator was also within ±20 percent. Since there were a few exceptions to these typical variations, tubing samples to be destructively analyzed were surveyed with a radioactivity detector to ensure that a representative sample was taken.

- The Co-60 on the tubes increased with time of plant operation up to about 9 EFPY. The trend of the increase was similar to that calculated by the CORA code except that CORA values were about 50 percent lower than those observed. The Co-58 observed values were quite scattered and no trend was apparent; however, the CORA-calculated value fell within the range of the data.

- A comparison between the activity on the straight length of tubing versus that on U-bend tubing indicated that the activity on U-bends is about twice that on straight tubes.

- There was not a good correlation between the steam generator channel head exposure rates and the Co-60 activity on the tubing from the same steam generator.

- In general, the chemical composition of the material descaled from the tubes approached that of the Inconel tubing as subsequent descalings were made. Most of the material and activity was removed in the first descaling. The percentage of chromium and iron was somewhat greater and the percentage of nickel less in the descaled material compared to that in the base metal. The nickel-to-iron ratio in the tubing crud was about 1.0, compared to a ratio of about 0.5 in typical core crud deposits.

- The percentage of cobalt in the descaled material was about ten times that in the Inconel tubing.

- The surface concentration of the descaled material was found to increase with EFPY at a rate of 8.5 mg/dm^2 per EFPY or 0.70 mg/dm^2-mo. This value represents the corrosion plus deposition rate less the corrosion release rate of the Inconel tubing. Using a nominal value of 3 mg/dm^2-mo for the corrosion rate of Inconel, the corrosion release rate was estimated to be 2.5 mg/dm^2-mo.

- The Fe-55, Co-60, and Mn-54 crud specific activity of the descaled material in μCi/mg of material removed in the first descaling decreased with operating time. This trend was also calculated by the CORA code. The Co-60, Mn-54, and Co-58 crud specific activity also decreased with the second and third descaling. For Mn-54 and Co-58, a similar decrease was noted in terms of specific activity per mg of parent. However, for Co-60, a similar decrease did not occur.

- Autoradiographs of the tubing material showed that it was uniformly distributed, with a few "hot spots." EDAX analyses of the surface of the material, as well as the surface underneath the hot spots, showed that its composition was primarily iron, nickel, and chromium. Since the spots are transparent to X-rays, they are believed to be boric acid.

- SEM images of tube crud showed a pattern of cracks presumably following the grain boundaries of the tubing material. However, the sizes of the boundaries of the tube crud were greater than those on the tubing surface. The crud removed from the tube surfaces appeared to comprise irregularly shaped flakes varying in size from 30 microns down to several microns in diameter.

- The average thickness of the tube crud was about 1 micron and the average apparent density was about 3.9 g/cm^3. This compares to an average density of about 1.2 g/cm^3 for core crud deposits.

- It seems likely that crud on steam generator tubes contain two distinct phases: metallic nickel and a mixed spinel, probably of the general composition $Ni_xFe_y(Co,Mn)_z\ Cr_{3-x-y-z}O_4$, where the values of x, y, and z may vary axially in the deposit on a given tube.

Section 5

RECOMMENDATIONS

The following recommendations are made based on the work discussed in this report:

- Determination of surface activities using gamma spectroscopy should continue when additional tubes are received. This determination will provide information about the Co-58 and longer-lived nuclides in a timely manner and will add to the existing data base.

- Since only six tubes were sampled in this program, characterization of tube crud similar to that performed should be done on additional tube samples. The tubes sampled also represented exposures clustered around 2 and 7 EFPY operation. Thus, additional data are needed to complete the time relationship of deposit behavior.

- Additional evaluation of the data using the CORA code should be performed in an effort to provide better matches to the data and insight into some of the transport parameters used in CORA.

- Samples of additional tubes in storage should be descaled and the removed material and tubes analyzed for cobalt. These data will provide additional information on the relationship between the percentage of cobalt in the descaled material and that in the tubing.

- A series of mixed spinels should be prepared in the laboratory and characterized to further determine the exact composition of tubing crud.

- Analyses for additional nuclides, such as Ni-63, and use of other techniques to define crystallite size should be performed on crud samples. This information should further aid in defining mechanisms of activity transport.

Section 6

REFERENCES

1. S. Kang, Y. Solomon, and M. Troy. An Evaluation of the Effectiveness of Reactor Coolant High-Temperature Filtration in Reducing Radiation Exposure. Palo Alto, CA: Electric Power Research Institute, forthcoming.

2. C. W. Vernon. Steam Generator Dose Rates on Westinghouse Pressurized Water Reactors. Palo Alto, CA: Electric Power Research Institute, June 1982, NP-2453.

3. D. D. Whyte, Internal communication.

4. C. A. Bergmann, et al. Evaluation of Cobalt Sources in Westinghouse-Designed Three- and Four-Loop Plants. Palo Alto, CA: Electric Power Research Institute, NP-2681, October 1982.

5. S. Hilpert and A. Wille. "Zusammenhänge Zwischen Ferromagnetismus und Aufbau der Ferrite." Z. für Physik. Chem. 18B, 1932, p. 291.

6. A. B. Johnson, et al. "Nature of Deposits on BWR and PWR Primary System Surfaces -- Relation to Decontamination," in Water Chemistry of Nuclear Reactor Systems 2. London: British Nuclear Energy Society, 1981.

Appendix A

SUMMARY OF IN SITU RADIOACTIVITY DATA

This appendix lists details of the tubing sampled for this work, and some data from previous work, typical variations of tubing activities, and details of nuclide activities in various descaling fractions.

Table A-1

STEAM GENERATOR TUBING IN SITU ACTIVITY[a]

Plant	EFPY	Average Co-60 Activity ($\mu Ci/cm^2$)	Average Co-58 Activity ($\mu Ci/cm^2$)	Co-58/Co-60 Ratio	Average Measured Generator Channel Head Exposure[b] Rate (R/hr)
1	0.56	0.65	10.3	15.8	5
2	0.67	1.45	13.0	9.0	7
3	1.33	0.94	10.8	12.2	-
4	1.49	0.79	6.6	8.3	8
5	1.88	2.89	-	-	-
3	1.95	2.56	4.6	1.8	-
6	3.83	2.90	10.4	3.6	8

[a]Collected in 1973
[b]From Reference 2

Table A-2

DETAILS OF TUBES SAMPLED, IN SITU ACTIVITY,
AND STEAM GENERATOR EXPOSURE RATES

Plant	Tube	Section	Steam Generator	Tube Shape	Analysis	Shutdown Date	EFPY	Co-60 Activity ($\mu Ci/cm^2$)	Co-58 Activity ($\mu Ci/cm^2$)	Co-58/Co-60 Ratio	Average Measured Steam Generator Channel Head Exposure Rate[b] (R/hr)
A	R34C36	3-3A	C	Straight	3	6/26/74	2.12	2.81	-	-	13
	R43C33	SP-OA-1	C	Slight curve	3	6/26/74	2.12	1.45	-	-	13
	R36C37	4B	B	Straight	1,2,3	8/1/81	7.02	5.25	1.27	0.24	11
B	R1C25	-	D	U-bend	1,2,3	3/15/80	1.76	1.79			10
C	R9C31	Middle	A	Straight	3	2/1/74	2.65	1.91	-	-	-
	R25C47	2B	A	Straight	3	4/16/75	3.36	3.66	-	-	16
	R45C52	7	B	Straight	3	4/15/78	5.35	6.24	-	-	9
D	R1C5		A	U-bend	3	11/15/76	2.09	2.87	-	-	10
	R4C30	O-1	B	Straight	3	2/15/77	2.21	1.93	-	-	8
	R5C40	1A-1	A	Straight	1,3	2/15/77	2.21	2.17	-	-	11
E	R21C74	4	A	Straight	1,3	1/15/76	1.58	1.36	-	-	8
	R1C11		A	U-bend	3	11/15/76	2.26	5.04	-	-	19
	R3C63	3-28	A	Straight	3	11/15/76	2.26	1.63	-	-	19
	R2C42	O-1A	C	Straight	3	11/15/76	2.26	3.39	-	-	20
F	R20C73	7A	A	Straight	3	10/15/79	6.64	3.58	-	-	19
	R20C73	1A	A	Straight	3	10/15/79	6.64	10.8[a]	-	-	-
G	R18C37	C	A	Straight	1,2,3	4/15/80	5.96	3.94	-	-	8
	R18C37	D	A	Straight	3	4/15/80	5.96	2.73	-	-	8
	R15C73	3A	A	Straight	1,2,3	5/15/81	6.84	5.38	3.92	0.73	9
H	R25C72	4C	B	Straight	3	8/1/75	1.17	0.590	-	-	5
	R1C79	-	B	U-bend	3	6/15/76	1.90	1.76	-	-	15
I	Various	Various	C	Straight	3	4/16/82	0.33	0.23	2.48	10.8	-
J	R49C55	22-25	A	Straight	3	11/29/81	0.40	0.13	1.68	13.3	-
K	R12C46	Various	C	Straight	3	4/23/82	3.08	1.48	3.70	2.50	-
L	Various	Various	-	Straight	3	10/1/80	8.89	8.70	-	-	-

[a] Atypical data, not included in evaluation
[b] From Reference 2

Table A-3

TYPICAL STEAM GENERATOR TUBE MEASUREMENT VARIATIONS

Along Length of Tube, Plant H

Tube R25C72 Distance From Referenced End (cm)[a]	Measured Gross Activity at Indicated Tube Segment (μCi/cm)[a]					
	1	1A	2B	3A	4A	4C
15	3.47	-	3.11	2.99	3.80	3.89
30	3.72	-	3.61	3.35	3.43	3.91
45	3.42	-	3.74	3.32	3.43	3.73
60	3.32	-	3.36	3.90	3.87	-
75	-	-	3.68	3.64	3.34	-
90	-	-	3.37	3.75	-	-
105	-	-	3.21	3.07	-	-
120	-	-	3.42	3.86	-	-
135	-	-	3.35	3.40	-	-
150	-	-	-	2.12	-	-
20	-	3.46	-	-	-	-
40	-	4.29	-	-	-	-

Mean activity = 3.51 μCi/cm
Standard deviation of mean = 0.38
= 10.8% of mean

Between Tubes From the Same Steam Generator, Plant C

Tube, Segment	Measured Gross Activity at Center of Tube Length (μCi/cm)
R25C47,1	27.76
R25C47,2A	19.00
R25C47,2B	19.09
R20C24,3A	21.73
R20C24,3B	20.83

Mean activity = 21.68 μCi/cm
Standard deviation of mean = 3.60
= 16.6% of mean

[a]Smallest number is closest to tubesheet.

Table A-4

NUCLIDE ACTIVITIES IN DESCALED MATERIAL

				Co-60				Mn-54				Co-58			
Plant	EFPY	Descaling Run	Amount Descaled (mg)	Total μCi	μCi/ mg Crud	% Co	mCi/ mg Co	Total μCi	μCi/ mg Crud	% Fe	μCi/ mg Fe	Total μCi	μCi/ mg Crud	% Ni	μCi/ mg Ni
E	1.58	1	3.88	44.05	11.35	0.28	4.05								
		2	1.12	4.65	4.15	0.09	4.61								
		3	0.67	0.48	0.72										
B	1.75	1	4.04	48.58	12.02	0.22	5.46	7.59	1.88	14.5	13.0				
		2	1.02	4.23	4.15			0.57	0.56	9.2	6.1				
		3	1.01	1.70	1.68			0.24	0.24	9.2	2.6				
D	2.21	1	6.07	65.44	10.78	0.26	4.15								
		2	0.70	5.25	7.50										
		3	0.61	3.29	5.34										
G	5.96	1	15.44	109.76	7.11	0.12	5.93	7.93	0.51	20.4	2.5				
		2	2.99	16.11	5.39	0.09	5.99	0.91	0.30	15.7	1.9				
		3	0.72	2.12	2.94			0.14	0.19	15.8	1.2				
G	6.84	1	11.94	180.87	15.15	0.20	7.58	5.18	0.43	20.0	2.2	137.65	11.53	23.1	49.9
		2	0.67	5.95	8.88	0.22	4.04	0.22	0.33	18.2	1.8	4.73	7.06	30.4	23.2
		3	0.28	0.56	1.96	0.09	2.18	0.02	0.07	10.2	0.7	0.42	1.50	43.0	3.5
A	7.02	1	13.86	123.55	8.91	0.36	2.48	1.68	0.12	14.8	0.8	23.48	1.69	39.0	4.34
		2	9.53	57.87	6.07	0.14	4.34	0.87	0.09	15.9	0.6	12.58	1.32	38.2	3.46
		3	4.80	5.46	1.14	0.04	2.85	0.05	0.01	8.9	0.1	0.98	0.20	50.4	0.40

Appendix B

AS-COLLECTED ACTIVITY MEASUREMENTS

This appendix presents activity data from all tubes sampled under this work. The measurements are corrected for decay, and are given in units of either μCi Co-60/cm of tube length or in mR/hr. To convert to $\mu Ci/cm^2$, the following factors apply:

Plant	Divide By
A	6.58
C	6.58
E	6.58
H	6.58
I	5.54
J	5.54
K	6.58
L	5.54

Table B-1

STEAM GENERATOR TUBE ACTIVITY MEASUREMENTS

Plant: E
Date analyzed: December 1, 1981

Tube: R21C74
Steam generator: A
Removal date: January 1976

Section 2, cold leg, 276 cm of tube length

Distance From End of tube (cm)	Co-60 Activity (μCi/cm length)
45	9.38
60	9.97
75	8.45
90	11.42
105	9.81
120	9.78
135	11.06
150	11.68
165	11.12
180	11.11
195	9.26
210	10.97
225	14.32
240	10.67

Section 4, cold leg, 228 cm of tube length

Distance From End of Tube (cm)	Co-60 Activity (μCi/cm length)
30	9.27
45	10.95
60	9.36
75	9.01
90	10.30
105	9.82
120	11.30
135	11.57
150	10.44
165	11.26
180	9.34

Table B-1 (cont)

STEAM GENERATOR TUBE ACTIVITY MEASUREMENTS

Section 3, cold leg, 270 cm of tube length

Distance From End of Tube (cm)	Co-60 Activity (μCi/cm length)
30	8.73
45	11.34
60	9.65
75	10.39
90	-
105	10.25
120	9.93
135	8.34
150	10.11
165	9.76
180	8.58
195	10.37
210	10.11
225	10.63

Section 1 (in four parts), cold leg

Distance From End of Tube (cm)	Co-60 Activity (μCi/cm length)	
30	10.63	(88 cm of tube length)
45	12.42	
60	10.37	
4	2.63	(57 cm of tube length)
19	13.42	
34	17.28	
49	13.23	
30	13.83	(98 cm of tube length)
45	19.81	
60	15.82	
30	13.66	(141 cm of tube length)
45	-	
60	11.00	
75	9.98	
90	10.17	
105	9.15	
120	10.96	

Table B-1 (cont)

STEAM GENERATOR TUBE ACTIVITY MEASUREMENTS

Plant: C
Date analyzed: December 1, 1981

Tube: R9C31
Steam generator: A
Removal date: February 1974

Midsection, cold leg, 58 cm of tube length

Distance From End of Tube (cm)	Co-60 Activity (μCi/cm length)
4	12.39
19	14.48
35	16.63
49	13.98

Top section, cold leg, 45.5 cm of tube length

Distance From End of Tube (cm)	Co-60 Activity (μCi/cm length)
4	18.80
19	18.30
35	13.66

Top section, hot leg, 7.9 cm of tube length

Location	Co-60 Activity (μCi/cm length)
Middle of segment	16.74

Tube: R19C23
Steam generator: A
Removal date: February 1974

Section 1A, cold leg, 16 cm of tube length

Location	Co-60 Activity (μCi/cm length)
Middle of segment	12.44

Table B-1 (cont)

STEAM GENERATOR TUBE ACTIVITY MEASUREMENTS

Tube: R25C47
Steam generator: A
Removal date: April 1975

Section 1, hot leg, 24.5 cm of tube length

Location	Co-60 Activity (μCi/cm length)
Middle of segment	27.76

Section 2A, hot leg, 9 cm of tube length

Location	Co-60 Activity (μCi/cm length)
Middle of segment	19.00

Section 2B, hot leg, 17.5 cm of tube length

Location	Co-60 Activity (μCi/cm length)
Middle of Segment	19.09

Tube: R20C24
Steam generator: A
Removal date: April 1975

Section 3A, hot leg, 9.3 cm of tube length

Location	Co-60 Activity (μCi/cm length)
Middle of segment	20.83

Section 3B, hot leg, 12.7 cm of tube length

Location	Co-60 Activity (μCi/cm length)
Middle of segment	21.73

Table B-1 (cont)

STEAM GENERATOR TUBE ACTIVITY MEASUREMENTS

Plant: A
Date analyzed: December 1, 1981

Tube: R34C36
Steam generator: C
Removal date: June 1974

Section 1-1A, 10 cm of tube length

Location	Co-60 Activity (μCi/cm length)
Middle of segment	15.64

Section 1B-2, 39 cm of tube length

Location	Co-60 Activity (μCi/cm length)
Middle of Segment	17.10

Section 3-3A, 45 cm of tube length

Distance From End of Tube (cm)	Co-60 Activity (μCi/cm length)
15	14.40
30	16.36

Section 3D-4, 17.4 cm of tube length

Location	Co-60 Activity (μCi/cm length)
Middle of segment	14.14

Section 4-5, 25.4 cm of tube length

Location	Co-60 Activity (μCi/cm length)
Middle of segment	14.70

Table B-1 (cont)

STEAM GENERATOR TUBE ACTIVITY MEASUREMENTS

Tube: R43C33
Steam generator: C
Removal date: June 1974

Section SP-OA-1, U-bend, 14.4 cm of tube length

Location	Co-60 Activity (μCi/cm length)
Middle of segment	7.49

Section AVB-O-OA, U-bend, 10 cm of tube length

Location	Co-60 Activity (μCi/cm length)
Middle of segment	6.31

Section AVB-O-OB, U-bend, 5.8 cm of tube length

Location	Co-60 Activity (μCi/cm length)
Middle of segment	6.53

Plant: H
Date analyzed: December 30, 1981

Tube: R25C72
Steam generator: B
Removal date: August 1975

Section 1, hot leg, 80.6 cm of tube length

Distance From End of Tube (cm)	Co-60 Activity (μCi/cm length)
15	3.47
30	3.72
45	3.42
60	3.32

Table B-1 (cont)

STEAM GENERATOR TUBE ACTIVITY MEASUREMENTS

Section 2B, hot leg, 147.7 cm of tube length

Distance From End of Tube (cm)	Co-60 Activity (μCi/cm length)
15	3.11
30	3.61
45	3.74
60	3.63
75	3.68
90	3.73
105	3.21
120	3.42
135	3.35

Section 3A, hot leg, 160.5 cm of tube length

Distance From End of Tube (cm)	Co-60 Activity (μCi/cm length)
15	2.99
30	3.35
45	3.32
60	3.90
75	3.64
90	3.75
105	3.07
120	3.86
135	3.40
150	2.12

Section 4A, hot leg, 89.5 cm of tube length

Distance From End of Tube (cm)	Co-60 Activity (μCi/cm length)
15	3.80
30	3.43
45	3.43
60	3.87
75	3.34

Section 4C, hot leg, 64.8 cm of tube length

Distance From End of Tube (cm)	Co-60 Activity (μCi/cm length)
15	3.89
30	3.91
45	3.73

Table B-1 (cont)

STEAM GENERATOR TUBE ACTIVITY MEASUREMENTS

Section 1A 10FZ, cold leg, 57.5 cm of tube length

Distance From End of Tube (cm)	Co-60 Activity (μCi/cm length)
20	3.46
40	4.29

Section 1A 20FZ, cold leg, 4.5 cm of tube length

Location	Co-60 Activity (μCi/cm length)
Middle of segment	2.12

Section 1B, cold leg, 5.7 cm of tube length

Location	Co-60 Activity (μCi/cm length)
Middle of segment	1.98

Table B-2

UNCOLLIMATED G-M SURVEY MEASUREMENTS

Date of survey: December 1981

Plant	Tube	Section	Steam Generator	Length of Tube (in.)	Location	Removal Date	Radiation Level (mR/hr)
A	R36C37	4B	B	10.5	Hot leg	8/81	180, 180[a]
C	R45C52	3A	B	8	Hot leg	4/78	110, 110[a]
		7	B	12	Hot leg	4/78	140, 140[a]
		10C	B	16	Hot leg	4/78	140, 140[a]
D	R4C30	7C	B	16.5	Hot leg	2/77	100, 100[b]
		O-1,A	B	14.3	Hot leg	2/77	70, 70[b]
		O-1,B	B	9.3	Hot leg	2/77	70, 70 (on contact, 2 in. from each end)
	R5C40	1A-1	A	16	Hot leg	2/77	110, 110[b]
		10A-1	A	16	Hot leg	2/77	100, 100[b]
E	R3C63	3-2B	A	10.125	Cold leg	11/76	60, 60[b]
	R2C42	O-1A	C	16	Hot leg	11/76	100, 100[c]
		1-2A	C	16	Hot leg	11/76	80, 80[c]
F	R20C37	7A	A	16	Hot leg	10/79	100, 100[c]
		1A	A	13	Hot leg	10/79	175, 200 (at 4 in. from each end, probe 3.5 in. from tube)
G	R18C37	C	A	4.5	Hot leg	4/80	90 } at center of tube
		D	A	3.4	Hot leg	4/80	50 } length, probe 1.5 in. away
	R15C73	3A	A	16	Hot leg	5/81	200, 200[b]
B	R1C19	--	D	--	U-bend	3/80	20[d]
	R1C9	--	D	--	U-bend	3/80	20[d]
	R1C25	--	D	--	U-bend	3/80	20[d]
D	R1C11	--	A	--	U-bend	11/76	40[d]
	R1C5	--	A	--	U-bend	11/76	20[d]
H	R1C79	--	B	--	U-bend	6/76	12[d]
	R1C78	--	B	--	U-bend	6/76	12[d]

[a]Measurement taken 2 inches from each end of tube with probe 1.5 inches away
[b]Measurement taken 4 inches from each end of tube with probe on contact
[c]Measurement taken 4 inches from each end of tube with probe 1.5 inches away
[d]Probe 3.5 inches from outer bend area

Table B-3

STEAM GENERATOR TUBE Co-58 AND Co-60 MEASUREMENTS

Date Analyzed: June 23, 1982

Plant	Tube	Section	Steam Generator	Location	Shutdown Date	Length of Tube (cm)	Co-60 Activity (μCi/cm length)	Co-58 Activity (μCi/cm length)
I	R49C48	5	C	Hot leg	4/82	3.0	0.455	3.52
	R49C48	6	C	Hot leg	4/82	2.8	1.07	9.50
	R49C48	8	C	Hot leg	4/82	2.8	1.26	12.4
	R49C53	4	C	Hot leg	4/82	3.1	1.26	10.8
	R49C53	0-0A	C	Hot leg	4/82	15.3	1.62	12.4
	R49C53	0-0Z	C	Hot leg	4/82	15.3	1.47	12.8
	R49C53	5	C	Hot leg	4/82	2.5	0.454	3.35
	R49C42	5	C	Hot leg	4/82	8.1	0.544	2.96
J	R49C55	22-25	A	Cold leg	11/81	8.4	0.622	8.92
K	R12C46	1	C	Cold leg	4/82	30.8	8.79	21.5
	R12C46	2	C	Cold leg	4/82	64.7	9.37	20.7
	R12C46	2A	C	Cold leg	4/82	14.1	9.46	23.7
	R12C46	3	C	Cold leg	4/82	54.8	8.57	18.5
L	R10C51	5	--	--	10/80	68.3	29.2	--
		4	--	--	10/80	22.2	17.9	--
	R10C43	A	--	--	10/80	58.1	30.5	--
		2	--	--	10/80	41.8	8.20	--
	R22C84	3	--	--	10/80	45.0	35.6	--
		2	--	--	10/80	50.7	37.8	--
	R17C45	3	--	--	10/80	71.4	37.8	--
	R41C46	2	--	--	10/80	29.0	23.1	--
	R25C80	3	--	--	10/80	50.0	38.4	--